NASA TN D-434

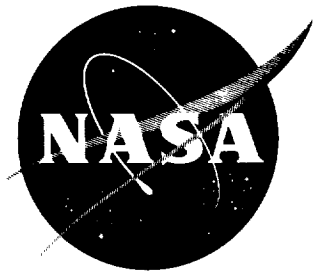

TECHNICAL NOTE
D-434

LOW-SPEED INVESTIGATION OF A FULL-SPAN INTERNAL-FLOW JET-AUGMENTED FLAP ON A HIGH-WING MODEL WITH A 35° SWEPT WING OF ASPECT RATIO 7.0

By Thomas R. Turner

Langley Research Center
Langley Field, Va.

NATIONAL AERONAUTICS AND SPACE ADMINISTRATION
WASHINGTON
August 1960

NATIONAL AERONAUTICS AND SPACE ADMINISTRATION

TECHNICAL NOTE D-434

LOW-SPEED INVESTIGATION OF A FULL-SPAN INTERNAL-FLOW JET-AUGMENTED FLAP ON A HIGH-WING MODEL WITH A 35° SWEPT WING OF ASPECT RATIO 7.0

By Thomas R. Turner

SUMMARY

An investigation of a full-span 17-percent-chord internal-flow jet-augmented flap on an aspect-ratio-7.0 wing with 35° of sweepback has been made in the Langley 300-MPH 7- by 10-foot tunnel. Blowing over the conventional elevator and blowing down from a nose jet were investigated as a means of trimming the large diving moments at the high momentum and high lift coefficients.

The results of the investigation showed that the model with the horizontal tail 0.928 mean aerodynamic chord above the wing-chord plane was stable to the maximum lift coefficient. The large diving-moment coefficients could be trimmed either with a downward blowing nose jet or by blowing over the elevator. Neither the downward blowing nose jet nor blowing over the elevator greatly affected the static longitudinal stability of the model. Trimmed lift coefficients up to 8.8 with blowing over the elevator and up to 11.4 with blowing down at the nose were obtained when the flap was deflected 70° and the total momentum coefficients were 3.26 and 4.69.

INTRODUCTION

In previous investigations jet-augmented flaps have shown promise in reducing the take-off and landing velocity and distance of jet aircraft. (For example, see refs. 1, 2, and 3.) The large lift increases produced by the jet flap are accompanied by large pitching moments that have to be trimmed by some means. Large lift losses occur as a wing equipped with a jet flap operating at a high lift coefficient approaches the ground (ref. 4). Considering the ground effect and the large moments involved, it appeared that an airplane with a high wing, a high tail, and a rather long tail length would be a promising configuration for use with a jet-augmented flap.

The beneficial effect of a high horizontal tail on longitudinal stability was verified from an investigation of a partial-span jet-augmented flap on a high-wing model with a typical transport plan form (aspect ratio of 7.0, taper ratio of 0.3, 35° sweepback of 0.25-chord line) presented in reference 3. The present investigation used the same basic model equipped with a full-span 17-percent-chord plain jet-augmented flap. Data are presented for flap deflections from 0° to 70° with the momentum coefficient varying from 0 to approximately 6.33.

SYMBOLS

The coefficients of forces and moments are referred to the wind axes with the chordwise center of moments at 33 percent of the mean aerodynamic chord.

b	twice wing span of semispan model, ft
C_D	drag coefficient, D/qS
C_L	lift coefficient, L/qS
$C_{L,max}$	maximum lift coefficient
C_m	pitching-moment coefficient, $\frac{\text{Pitching moment}}{qS\bar{c}}$
$C_{\mu,n}$	nose momentum coefficient, $\frac{\text{Nose-jet static thrust}}{qS}$
$C_{\mu,t}$	tail momentum coefficient, $\frac{\text{Static thrust leaving elevator}}{qS}$
$C_{\mu,w}$	wing momentum coefficient, $m_j V_j/qS$
c	wing chord, ft
$\bar{c}$	mean aerodynamic chord, ft
D	drag, lb
F_r	redirected thrust (leaving trailing edge of flap), $\sqrt{L^2 + D^2}$ with $q = 0$
h	vertical distance of moment center from wing chord line, positive when above, units of $\bar{c}$

i_t	incidence of horizontal tail, positive with trailing edge down, deg
L	lift, lb
m_j	mass flow in jet, slugs/sec
q	free-stream dynamic pressure, $\rho V^2/2$, lb/sq ft
S	area of semispan wing, sq ft
V	free-stream velocity, ft/sec
V_j	jet velocity, isentropic expansion to free-stream static pressure, ft/sec
z	vertical distance of tail from wing-chord line extended, positive when above, units of $\bar{c}$
α	angle of attack corrected for jet-boundary effects, deg
α'	angle of attack of wing with respect to tunnel center line, deg
δ_e	elevator deflection, positive with trailing edge down, deg
δ_f	flap deflection, measured with respect to wing-chord plane, deg
δ_j	jet deflection angle measured with respect to fuselage reference line with q = 0, deg
δ_s	leading-edge slat deflection, deg
ρ	mass density of air, slugs/cu ft

APPARATUS AND MODEL

The investigation of full-span internal-flow jet-augmented flaps on a high-wing transport-type model was made in the Langley 300-MPH 7- by 10-foot tunnel. The investigation was made by means of the semispan technique with the tunnel ceiling serving as the reflection plane. The compressed air was brought onto the mechanical-balance frame through a long $1\frac{1}{2}$-inch-diameter steel pipe that acts as a weak spring (ref. 2). The tares or interactions introduced by this method are negligible. This mechanical balance system was used for the 21° and 57° flap deflections only. For the rest of the investigation a strain-gage balance

having greater sensitivity and having a built-in air supply tube that gave negligible tares was used. The use of this balance necessitated a slightly different vertical moment center than was used for the other balance, and the data are presented about these vertical moment centers (fig. 1).

A three-view drawing of the model is shown in figure 1. The wing had an aspect ratio of 7, a taper ratio of 0.3, a quarter-chord sweep of 35°, and a full-span 0.17c plain flap. The streamwise wing sections were NACA 65A414 at the root and NACA 65A410 at the tip. The plain flap (fig. 2) was hinged at the lower surface at the 0.83-chord line with the upper surface of the flap nose forming one side of the compressed-air exit slot. The slot gap varied from 0.018 inch at the root to 0.006 inch at the tip. The flap angle normal to the hinge line with respect to the wing-chord plane varied from 0° to 70°. The vane used on the wing leading edge had a St. Cyr airfoil section with a taper ratio of 0.3 (fig. 2). Two outboard vane spans, extending from the wing tip inboard to 0.40 $\frac{b}{2}$ and 0.57 $\frac{b}{2}$, were used in the investigation.

L 9 3 1

Details of the horizontal tail, which had an area of 32 percent of the wing area, are shown in figures 1 and 2. Data were obtained with the tail located 0.428$\bar{c}$, 0.928$\bar{c}$, and 1.428$\bar{c}$ above the wing-chord plane extended; however, most of the data were obtained at the 0.928$\bar{c}$ height.

A downward-exiting fuselage nose jet of 0.047$\bar{c}$ diameter located 2.48$\bar{c}$ ahead of the center of moments was used as a trim device for some of the tests (fig. 1).

TEST CONDITIONS

The tests were made at dynamic pressures varying from 1.5 to 20 pounds per square foot, with the Reynolds number varying from approximately 200,000 to 870,000 based on the mean aerodynamic chord of the wing. The value of wing momentum coefficient, based on measured mass flow and jet exit velocity, varied from 0 to approximately 3.10 for a free-stream dynamic pressure of 3.0. The jet exit velocity used in computing wing momentum coefficient was the average velocity over the length of the exit slot as determined from the temperature and pressure in the slot plenum chamber. The jet-flap exit gap had the same taper as the wing chord; therefore, each section of the wing would have operated at the same momentum coefficient if the plenum pressure had been constant across the span of the wing. The plenum chamber pressure was not linear across the flap span but tended to be higher over the center part of the reflection-plane wing. The ratio of spanwise plenum pressure to average plenum pressure used in computing $C_{\mu,w}$ is shown as a

function of spanwise distance along the flap hinge axis for two flap deflections in figure 3.

The jet turning angle as a function of flap deflection angle is presented in figure 4. These angles were determined from static (tunnel not operating) force tests and are average deflections.

CORRECTIONS

Jet-boundary corrections applied to the data were obtained by the method of reference 5. The magnitude of the corrections was determined by considering only the aerodynamic forces (circulation lift effects) on the model that resulted after the jet reaction components had been subtracted from the data as follows:

$$\alpha = \alpha' + 0.339\left[C_L - \frac{F_r}{qS}\sin\left(\delta_j + \alpha'\right)\right]$$

$$C_D = \left(C_D\right)_{measured} + 0.0053\left[C_L - \frac{F_r}{qS}\sin\left(\delta_j + \alpha'\right)\right]^2$$

Blocking corrections have not been applied to the data.

RESULTS AND DISCUSSION

Effects of Blowing Over Flap

The effect of $C_{\mu,w}$ on the model aerodynamic characteristics in pitch is presented in figure 5. The variation of $C_{\mu,w}$, C_D, and C_m with C_L at $\alpha' = 0^\circ$ for the model without the stabilizer is presented in figure 5(a) for the various flap deflections. These data show the usual effects, in that for a given flap deflection the larger lift gains occur for the lower $C_{\mu,w}$ values and increase with flap deflection. The pitching-moment coefficient increases (becomes more negative) almost linearly with lift coefficient and thus creates a real trim problem at the higher lift coefficients. Variations of the lift, drag, and pitching-moment coefficients through the angle-of-attack range for the model with stabilizer off and flap deflected 0°, and for the flap deflected 21° with stabilizer on and off, are presented in figures 5(b) and 5(c) for several

$C_{\mu,w}$ values. As is to be expected, the lift-curve slope increases with increased $C_{\mu,w}$, and $C_{L,max}$ is increased considerably more than the value of $C_{\mu,w}$. The drag coefficient near zero lift with the flap deflected 0° is reduced by approximately 70 percent of the $C_{\mu,w}$ value (fig. 5(b)). If account is taken of the fact that the blown air leaves the slot normal to the slot lip (or hinge line) and at an angle of approximately 30° to the plane of symmetry, the effective $C_{\mu,w}$ is reduced by 13 percent and the drag coefficient is reduced by approximately 80 percent of the streamwise $C_{\mu,w}$. These jet angles and also the possible effects of the spanwise velocity distribution of the jet should be considered when these data are used for thrust recovery studies.

Tail-Height Effects

The effects of tail-height variation on the pitch characteristics of the model for flap deflections of 21° and 57° at a wing momentum coefficient of 3.09 are presented in figure 6. The static longitudinal stability of the model for the 21° flap deflection is changed only slightly by increasing the tail height from $0.928\bar{c}$ to $1.428\bar{c}$ (fig. 6(a)). However, the C_m curve of the model for the $1.428\bar{c}$ tail height is linear to $C_{L,max}$, whereas there is a decrease in slope as $C_{L,max}$ is approached for the $0.928\bar{c}$ tail height. The stability of the model increases as the tail height is raised from $0.428\bar{c}$ to $0.928\bar{c}$ and to $1.428\bar{c}$ for the 57° flap configuration with elevator and stabilizer deflected (fig. 6(b)). There is only a very slight increase in the slope of the C_m curve for the $1.428\bar{c}$ height as compared with the $0.928\bar{c}$ height below a C_L value of approximately 7.5. Above a C_L value of 7.5 the slope of the C_m curve for the $0.928\bar{c}$ height approaches zero as $C_{L,max}$ is approached, whereas for the $1.428\bar{c}$ height the slope is practically unchanged up to $C_{L,max}$. Since a tail height of $1.428\bar{c}$ above the chord plane might be considered undesirable structurally for an operational aircraft, and since the model remained neutrally stable up to $C_{L,max}$ for the $0.928\bar{c}$ tail height, this location ($0.928\bar{c}$) was used for the bulk of the investigation.

Leading-Edge-Slat Characteristics

The effect of the wing leading-edge slat on the longitudinal characteristics of the model is presented in figures 7 and 8. The addition of the slat extended the linear part of the lift curve to higher angles of attack and also appreciably increased $C_{L,max}$. In general, the slat

delayed wing-tip stall (pitch-up) to wing maximum lift. The beneficial effects of the slat at the high flap deflections were increased with either an increased slat span or an increased slat deflection (fig. 8(b)).

Stabilizer Characteristics

Results from stabilizer tests for the various flap deflections at several values of $C_{\mu,w}$ are presented in figures 9 to 13, and the downwash characteristics are summarized in figure 14.

There were no particular peculiarities in any of the stabilizer test results for the various flap deflections and $C_{\mu,w}$ values. The stabilizer effectiveness dC_m/di_t varied from approximately -0.040 to -0.060 for the configurations tested. The average downwash angle at the tail ($z = 0.928\bar{c}$) varied from 2° to 29° for the various configurations as the lift coefficient varied from 0 to 10 (fig. 14). The average downwash at the tail for this model is primarily a function of the lift coefficient and is more or less independent of flap deflection, wing momentum coefficient, and angle of attack.

Trim Devices

As was pointed out previously, the diving moment for the model became very large at the high $C_{\mu,w}$ values and accompanying high lifts. Blowing over the deflected elevator is one method of trimming this moment. Results of blowing over the elevator deflected -60° with the wing flap deflected 57° and a $C_{\mu,w}$ value of 1.55, and with the wing flap deflected 57° and 70° and a $C_{\mu,w}$ value of 3.09, are presented in figures 12(a) and 15.

Deflecting the elevator -60° without blowing gives a positive pitching-moment coefficient increment of approximately 0.7 for the 57° flap deflection with a $C_{\mu,w}$ value of 3.09 (fig. 15(a)), whereas an increment of approximately 4.0 is required to trim at a C_L of 8.0. Blowing over the elevator with a $C_{\mu,t}$ value of 0.14 (based on wing area) gives a positive pitching-moment coefficient increment of approximately 2.5 and trims the model at a C_L value of 6.7. A $C_{\mu,t}$ value of 0.24 over the elevator trims the model at a C_L value of 7.7, which is close to 8.2, the $C_{L,max}$ value for the configuration (fig. 15(a)). Neither deflecting the elevator -60° nor blowing over the elevator appreciably changed the slope of the curve of pitching-moment coefficient plotted against lift coefficient for the test conditions.

A $C_{L,max}$ value of 10.3 was obtained with the wing flap deflected 70°, the stabilizer deflected 20°, and a $C_{\mu,w}$ value of 3.09 (fig. 15(b)). Deflecting the elevator -60° gives a positive pitching-moment increment of 0.7 which agrees with that for the 57° flap deflection. Blowing over the elevator with $C_{\mu,t}$ of 0.16 gives a positive pitching-moment coefficient increment of about 2.6 and a trim lift coefficient of 7.9. Increasing the tail momentum coefficient to 0.24 gives a trim lift coefficient of 8.8, as compared with 7.7 for the 57° flap. Blowing over the elevator of the configuration tested trims the configuration up to maximum lift for the $C_{\mu,w}$ range investigated, with approximately 10 percent loss in lift.

The model can be trimmed by means of a downward blowing nose jet without the large lift loss of the downward lifting tail if the necessary jet thrust is available at the nose. Results for a downward blowing nose jet located 2.48$\bar{c}$ ahead of the model center of moments for the wing flap deflected 70° with a $C_{\mu,w}$ value of 1.51 and 3.02 are presented in figure 16. The downward blowing nose jet increased the lift, the lift-curve slope, and the stall angle. At the lower angles of attack not all of the $C_{\mu,n}$ was recovered as lift; however, at the higher angles the increase in lift was larger than the downward $C_{\mu,n}$. Part of this lift increase is the result of a higher angle of attack for $C_{L,max}$ with the nose jet operating. Neither the slope of the curve of C_m plotted against C_L nor the stabilizer effectiveness is greatly affected by the downward blowing nose jet. The change in C_n produced by the downward blowing nose jet is in good agreement with the change computed as the product of $C_{\mu,n}$ and nose jet arm.

The conventional tail was sufficiently powerful to trim the model with the flap deflected 13° up to a C_L value of 3.5 with a $C_{\mu,w}$ value of 1.54 (fig. 17(a)). At the higher $C_{\mu,w}$ values blowing over the elevator was required to trim the model in pitch. The drag coefficient is negative up to $C_{L,max}$ for $C_{\mu,w}$ values of 1.54 and larger, a condition representing accelerating or climbing flight.

No data for the model trimmed in pitch were obtained with the wing flap deflected 21°. However, based on the tail-off moment (fig. 8(a)) and the tail effectiveness from the data for the 57° flap, it appears that a trimmed lift coefficient of approximately 5.8 (C_D approximately zero) can be obtained with a $C_{\mu,w}$ value of 3.09 and a $C_{\mu,t}$ value of about 0.13.

The conventional tail trims the model with the flap deflected 57° at a C_L value of 2.6 with a $C_{\mu,w}$ value of 0.14 (fig. 17(b)). A

momentum coefficient at the tail of 0.236 trims the configuration at a C_L value of 7.7 with a $C_{\mu,w}$ value of 3.09. At this same value of $C_{\mu,w}$ (3.09) with a downward $C_{\mu,n}$ value of 1.56 at the nose, a trim C_L value of 10.2 is obtained. These trimmed lift coefficients give approach angles up to approximately 9°; however, at an angle of attack of -20° with a total momentum coefficient of 3.15 the model will trim for a climb angle of approximately 13° at a C_L value of approximately 4.5.

Trimmed lift coefficients varied from approximately 3.6 to 11.4 for the model with flap deflected 70° (fig. 17(c)). All these configurations are stable (statically) in pitch from an angle of attack of -6° to the angle of attack for $C_{L,max}$. The trimmed lifts presented for the 70° flap are from 0 percent to about 20 percent higher than for the 57° flap at $C_{\mu,w}$ values from 0 to 3.0. The trimmed C_L values presented for the 70° flap give approach angles varying from 11° to 14° as compared with approach angles up to 9° for the 57° flap deflection.

Aerodynamically both methods of trimming the large diving moments produced by the highly deflected blowing flap are satisfactory. Both blowing down at the nose and blowing over the elevator trim the model, and the curves of C_m plotted against C_L are stable to the stall. However, it appears that for a total momentum coefficient up to approximately 2.0 a higher trim lift coefficient is obtained by blowing over the elevator. At the larger blowing quantities ($C_{\mu,w}$ above 2.0), blowing down at the nose gives a higher trim lift coefficient for the configuration investigated. In comparing the blowing tail and downward blowing nose jet data presented it should be remembered that the blowing-tail moment arm was $3.75\bar{c}$ as compared with $2.48\bar{c}$ for the nose jet.

SUMMARY OF RESULTS

A wind-tunnel investigation to determine the longitudinal characteristics of a high-wing transport model equipped with a full-span 17-percent-chord internal-flow jet-augmented flap has indicated the following results:

1. For a wing momentum coefficient of 3.09 and a flap deflection of 57° the static longitudinal stability of the model increased with increased tail height and was stable to the maximum lift coefficient for a tail height of $0.928\bar{c}$.

2. The leading-edge slat increased the maximum lift coefficient for all flap deflections and increased the static longitudinal stability near the maximum lift coefficient.

3. Trimmed lift coefficients up to 8.8 with blowing over the elevator and up to 11.4 with a downward blowing nose jet were obtained when the flap was deflected 70° with total momentum coefficients of 3.26 and 4.69.

Langley Research Center,
National Aeronautics and Space Administration,
Langley Field, Va., May 17, 1960.

REFERENCES

1. Lowry, John G., Riebe, John M., and Campbell, John P.: The Jet-Augmented Flap. Preprint No. 715, S.M.F. Fund Paper, Inst. Aero. Sci., Jan. 1957.

2. Lockwood, Vernard E., Turner, Thomas R., and Riebe, John M.: Wind-Tunnel Investigation of Jet-Augmented Flaps on a Rectangular Wing to High Momentum Coefficients. NACA TN 3865, 1956.

3. Turner, Thomas R., Davenport, Edwin E., and Riebe, John M.: Low-Speed Investigation of Blowing From Nacelles Mounted Inboard and on the Upper Surface of an Aspect-Ratio-7.0 35° Swept Wing With Fuselage and Various Tail Arrangements. NASA MEMO 5-1-59L, 1959.

4. Vogler, Raymond D., and Turner, Thomas R.: Wind-Tunnel Investigation at Low Speeds to Determine Flow-Field Characteristics and Ground Influence on a Model With Jet-Augmented Flaps. NACA TN 4116, 1957.

5. Gillis, Clarence L., Polhamus, Edward C., and Gray, Joseph L., Jr.: Charts for Determining Jet-Boundary Corrections for Complete Models in 7- by 10-Foot Closed Rectangular Wind Tunnels. NACA WR L-123, 1945. (Formerly NACA ARR L5G31.)

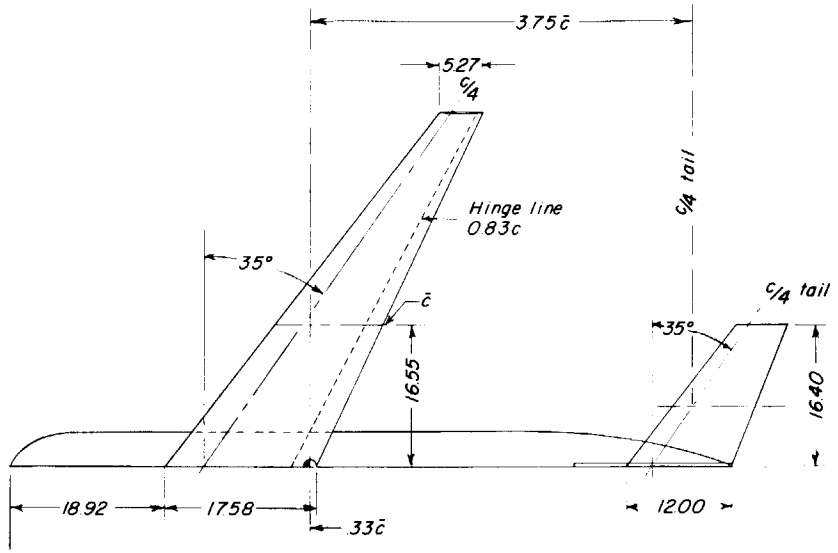

Wing	
Aspect ratio	7.0
Span	3.36 ft
Area	3.2 sq ft
Root chord	1.46 ft
Mean aerodynamic chord	1.044 ft
Airfoil section (parallel to airstream)	
Root section	65A 414
Tip section	65A 410
Leading edge sweep	37.83°
Incidence	0°
32.0% S horizontal tail	
Aspect ratio	3.64
Area	1.026 sq ft
Airfoil section	Modified flat plate

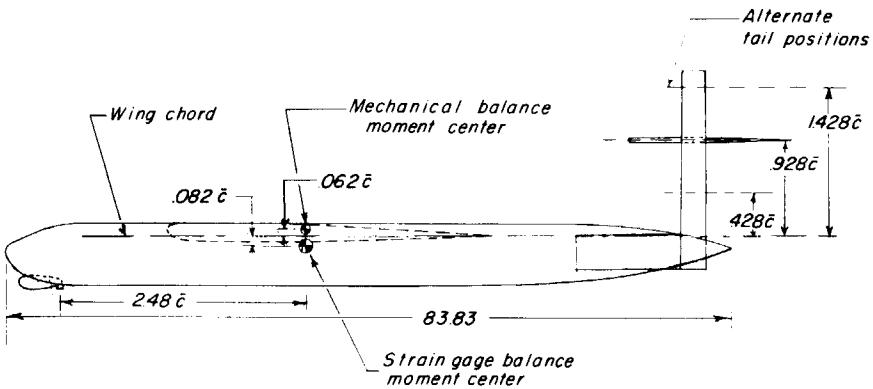

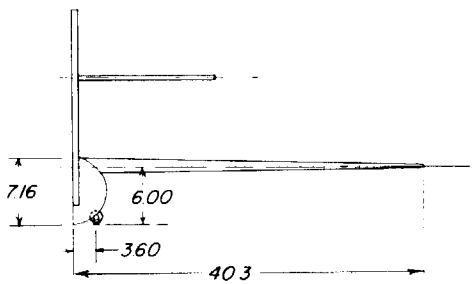

Figure 1.- Three-view drawing of model. Dimensions are in inches unless otherwise noted.

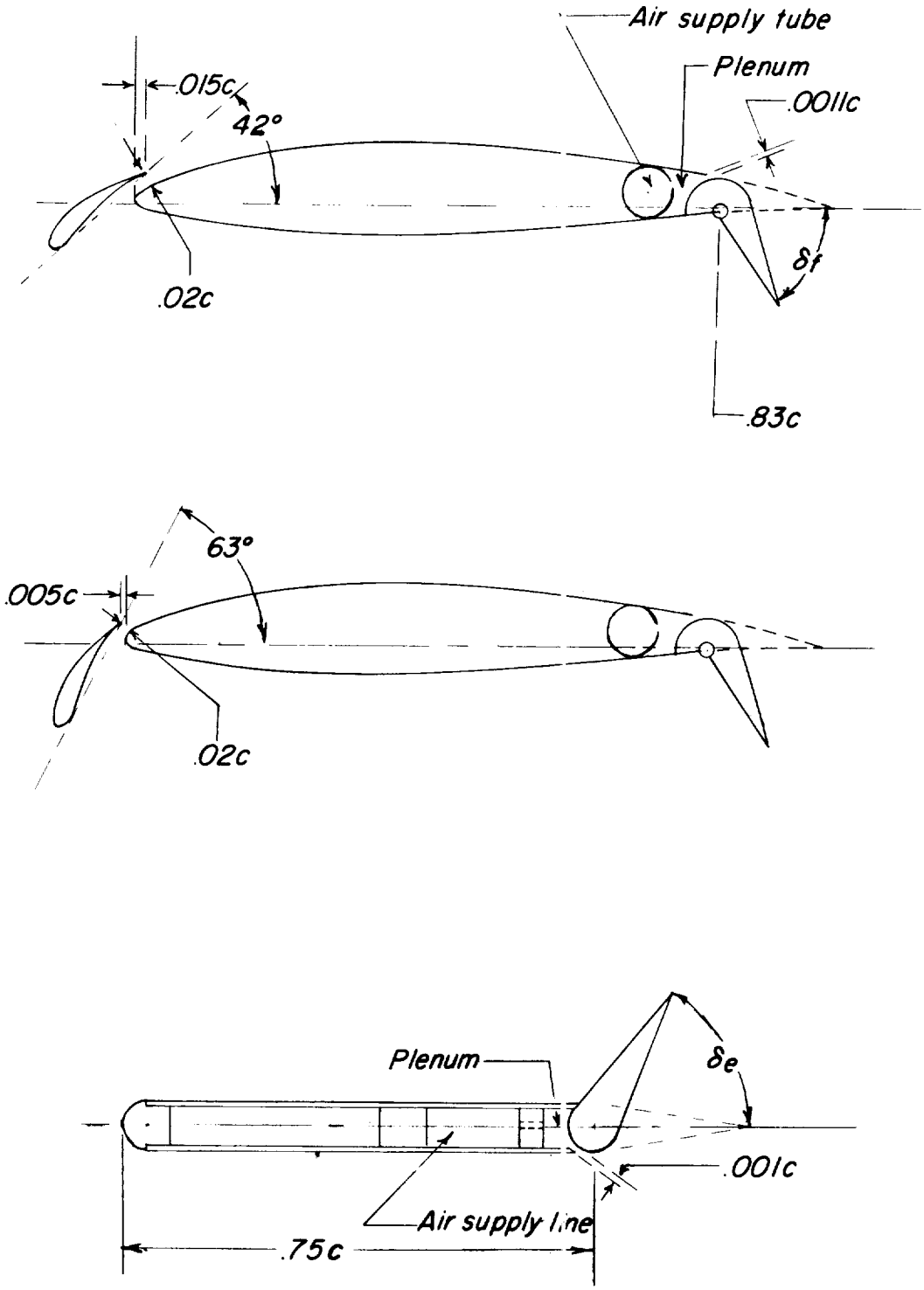

Figure 2.- Typical sections of the wing, flap, slats, and tail.

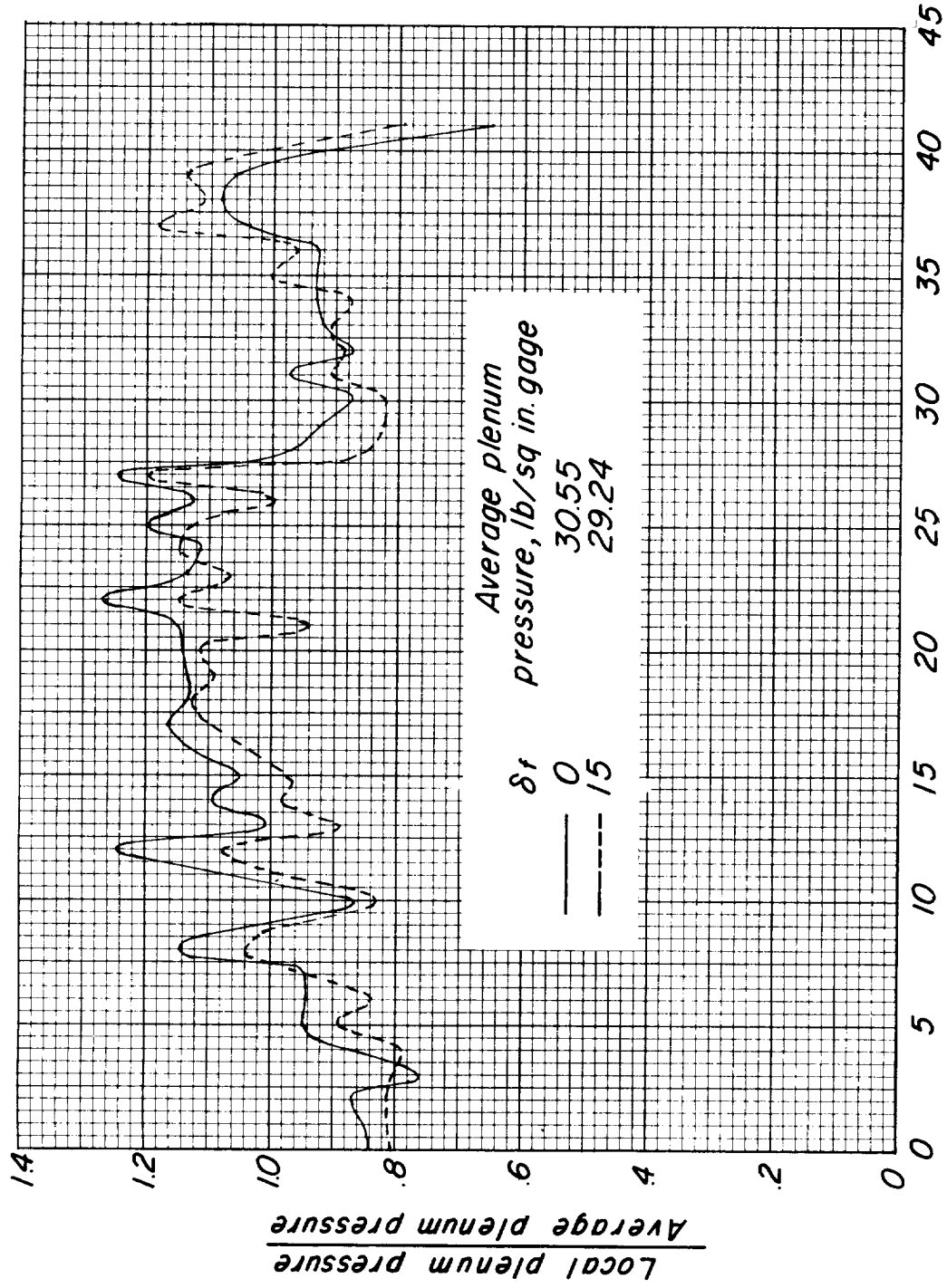

Figure 3.- Variation of plenum-chamber exit pressure across the span of the flap.

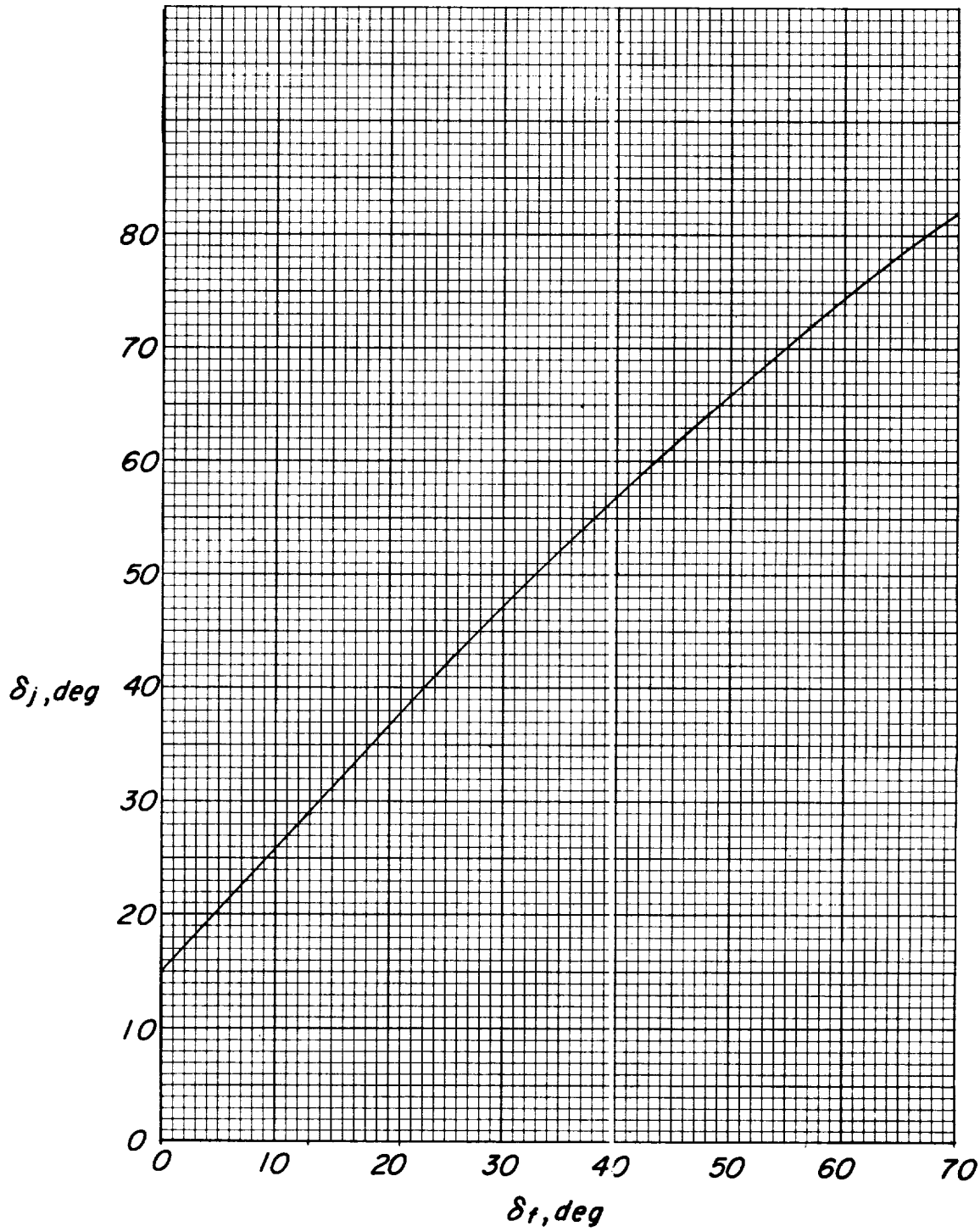

Figure 4.- Jet turning angle as a function of flap deflection.

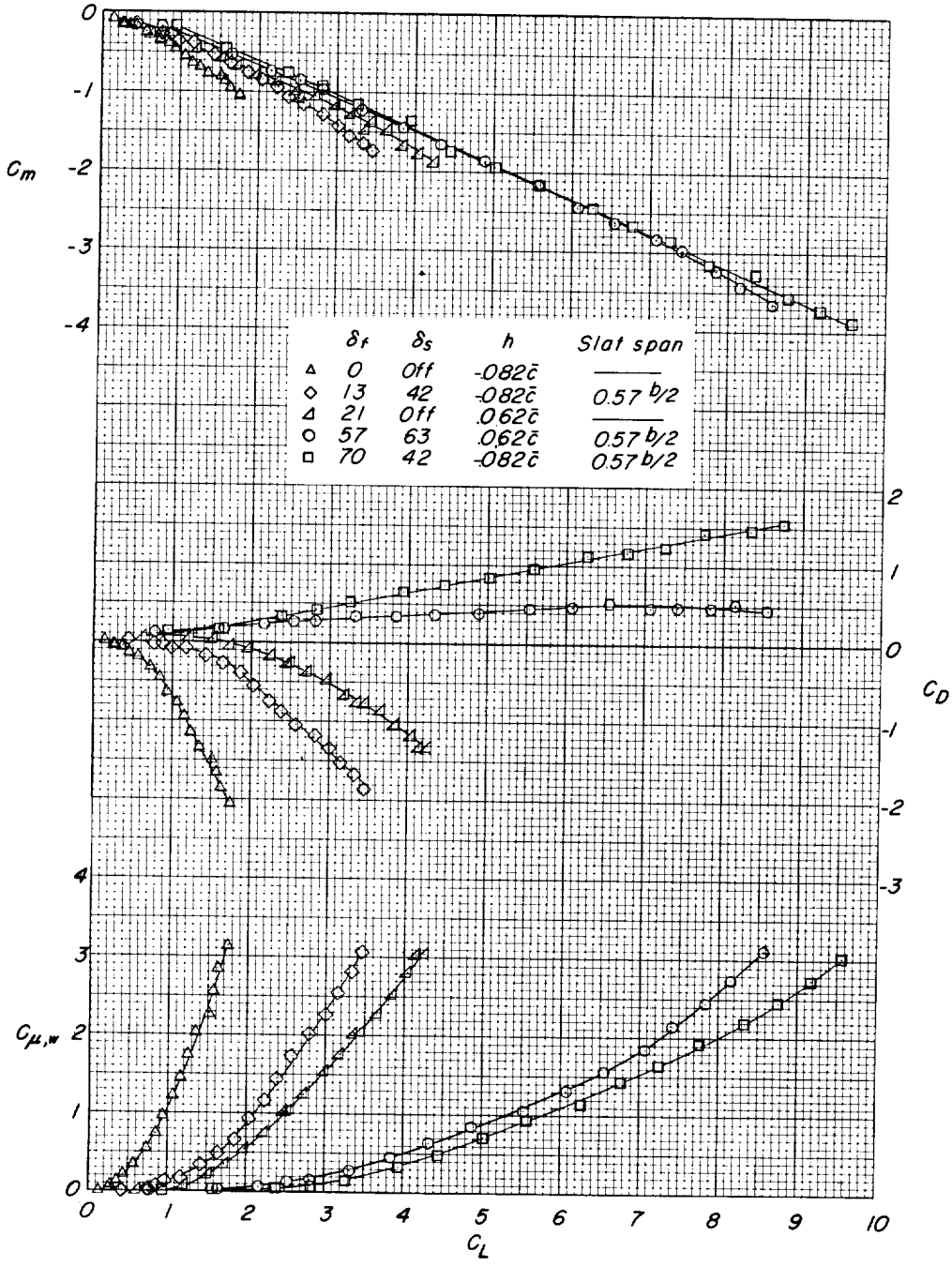

(a) $\alpha' = 0^\circ$; stabilizer off.

Figure 5.- Effect of momentum coefficient on the longitudinal aerodynamic characteristics of the model.

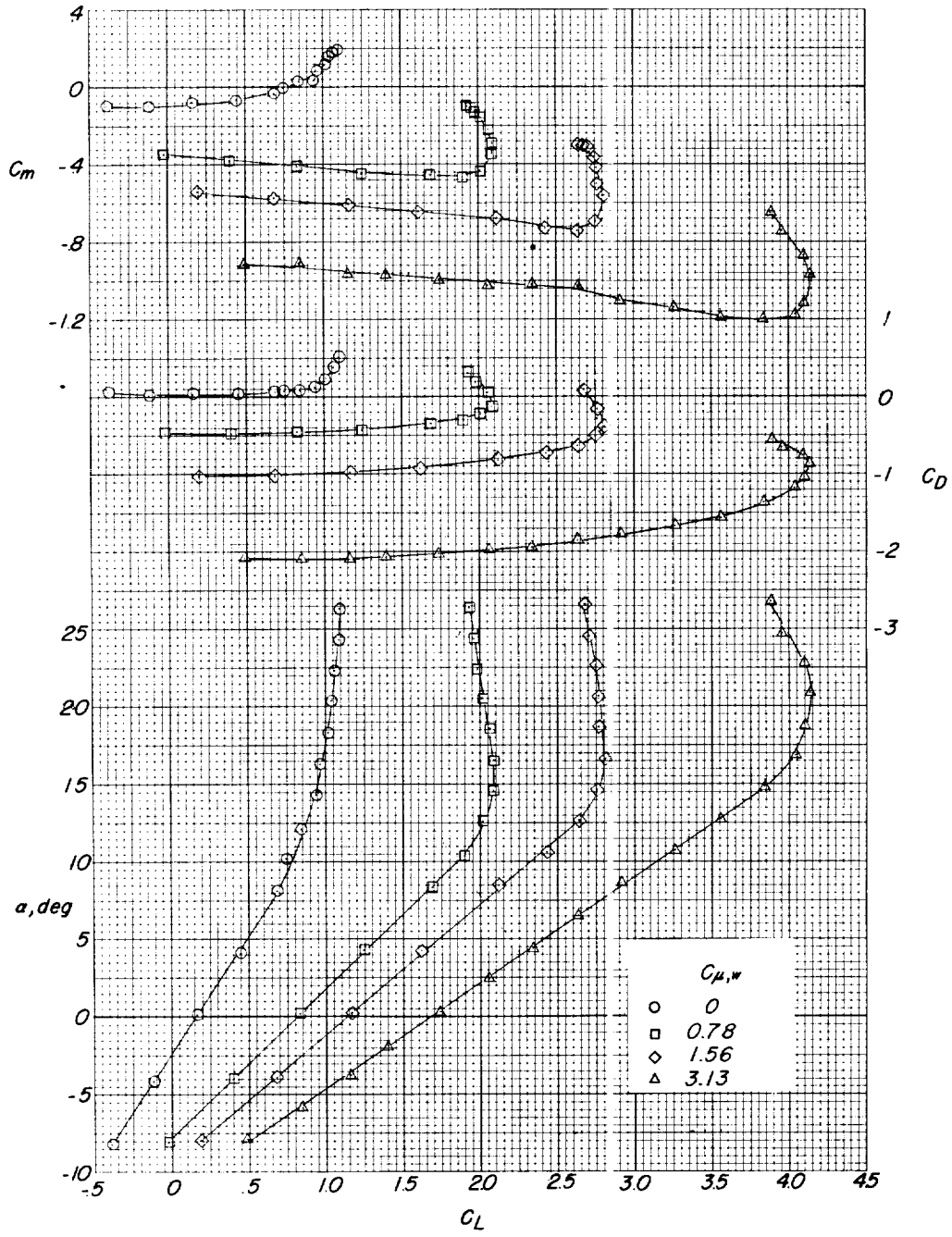

(b) $\delta_f = 0^o$; stabilizer off; slat off; h = -0.082$\bar{c}$.

Figure 5.- Continued.

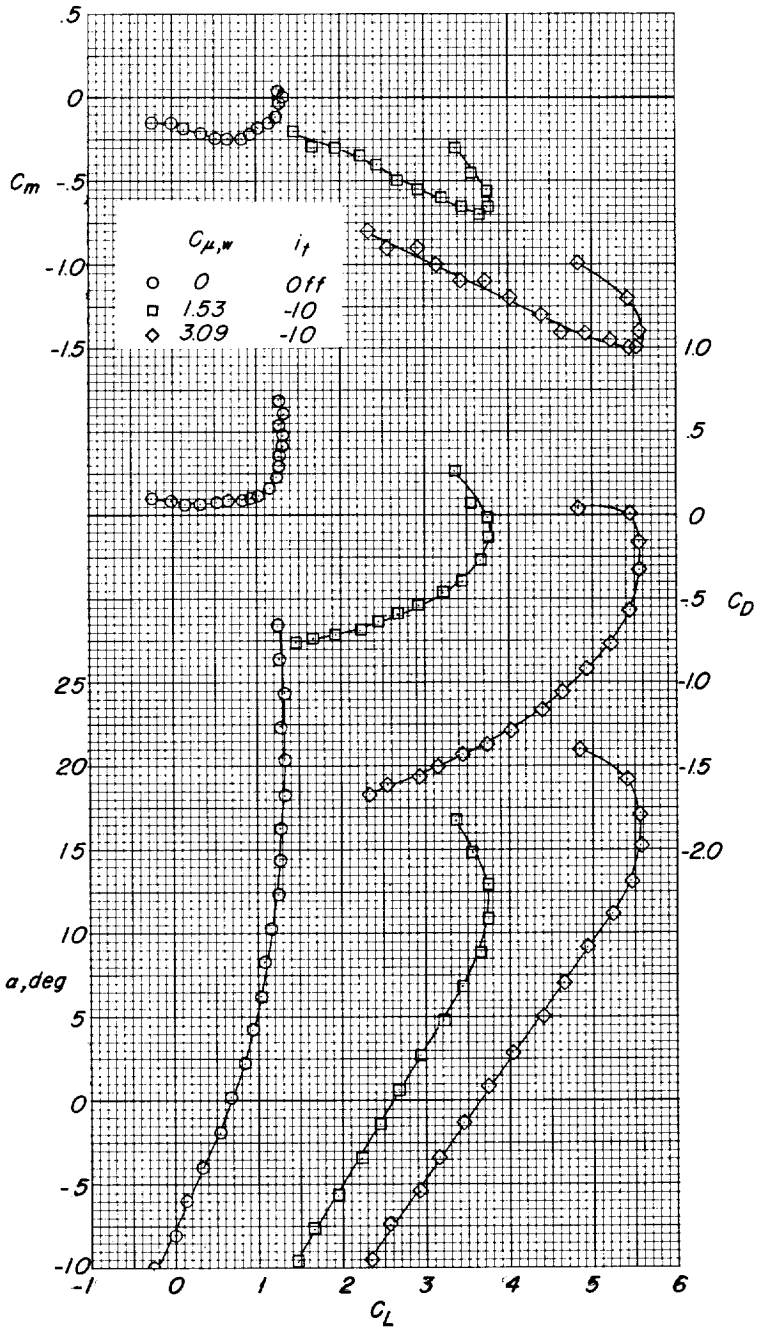

(c) $\delta_f = 21^\circ$; slat off; $z = 0.928\bar{c}$; $h = 0.062\bar{c}$.

Figure 5.- Concluded.

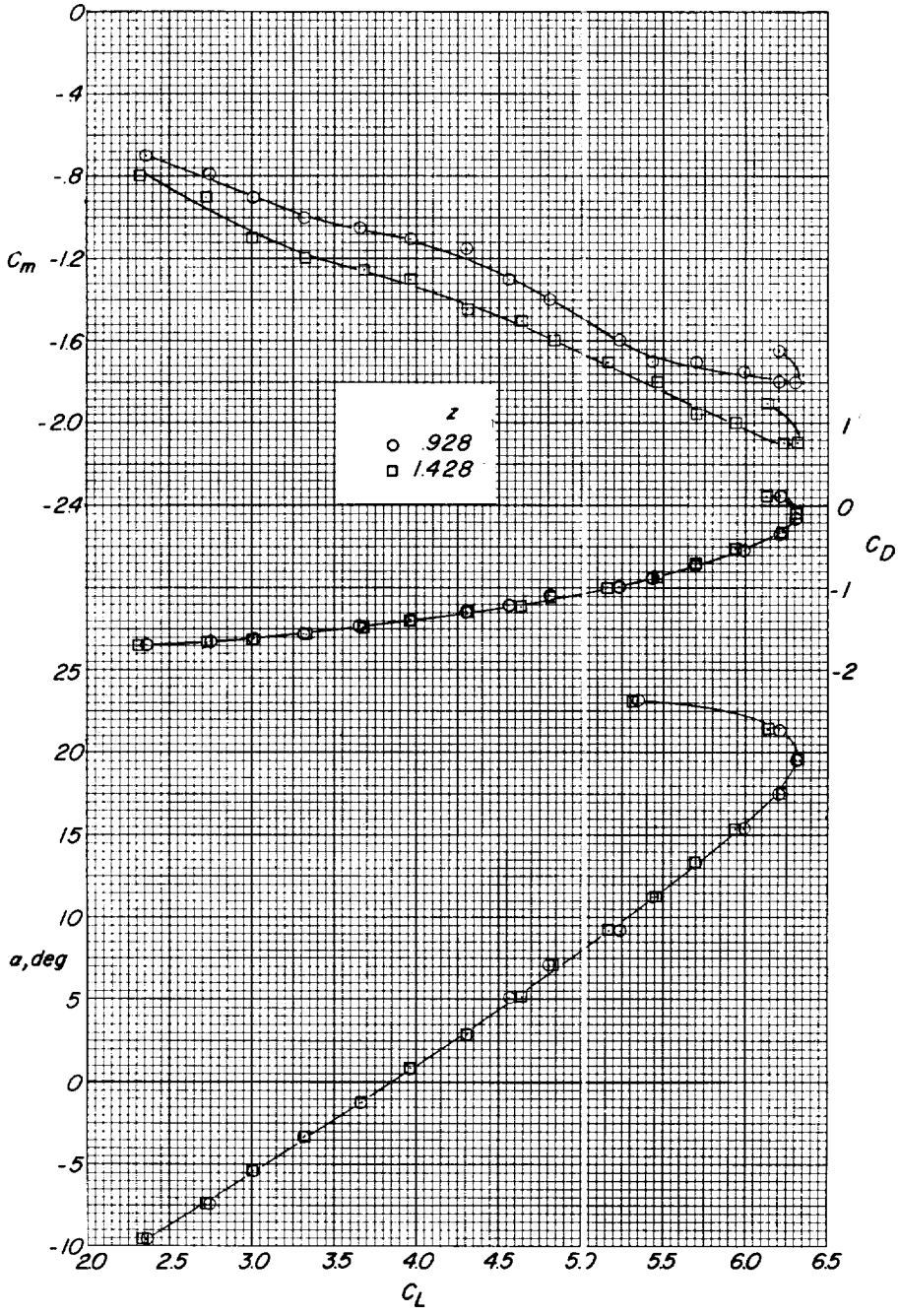

(a) $\delta_f = 21^\circ$; $i_t = 0^\circ$; $h = 0.062\bar{c}$.

Figure 6.- Effect of varying tail height on the pitch characteristics of the model. $C_{\mu,w} = 3.09$.

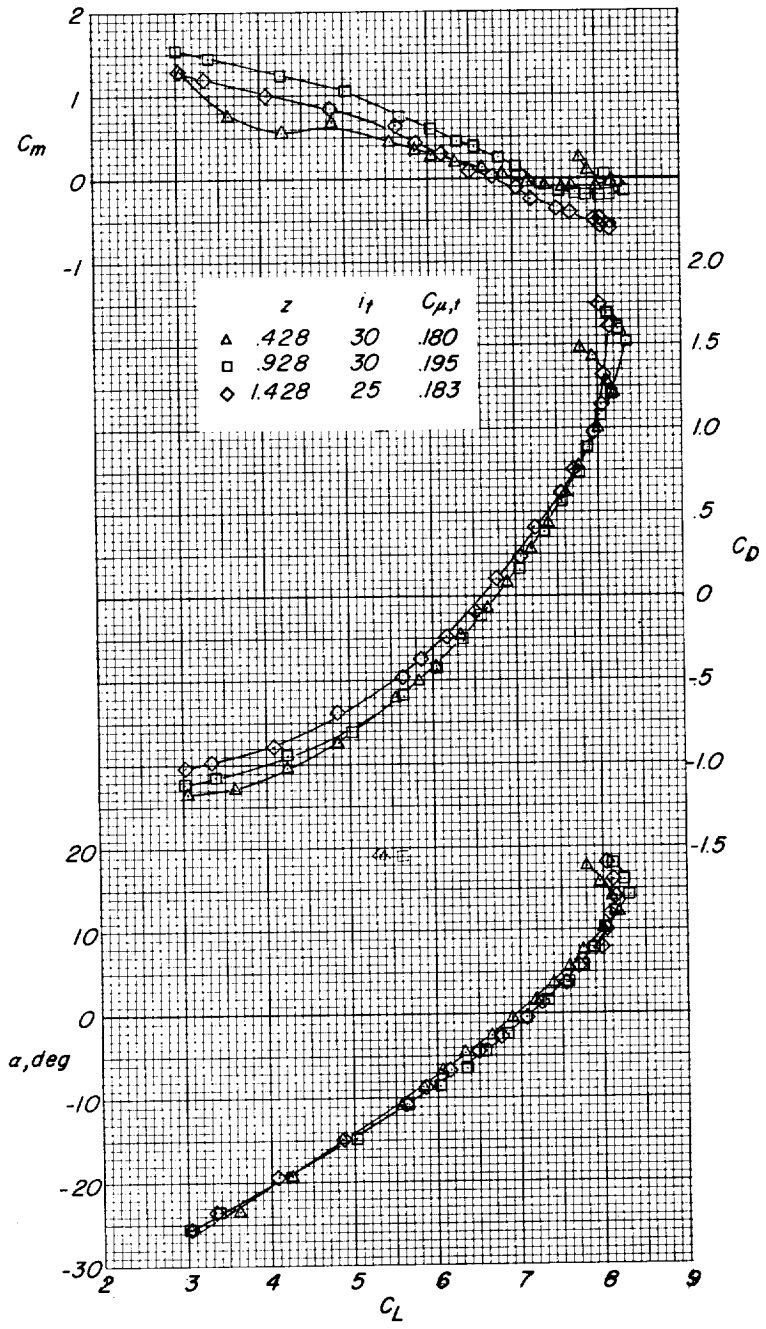

(b) $\delta_f = 57^\circ$; $\delta_e = -60^\circ$; $h = 0.062\bar{c}$.

Figure 6.- Concluded.

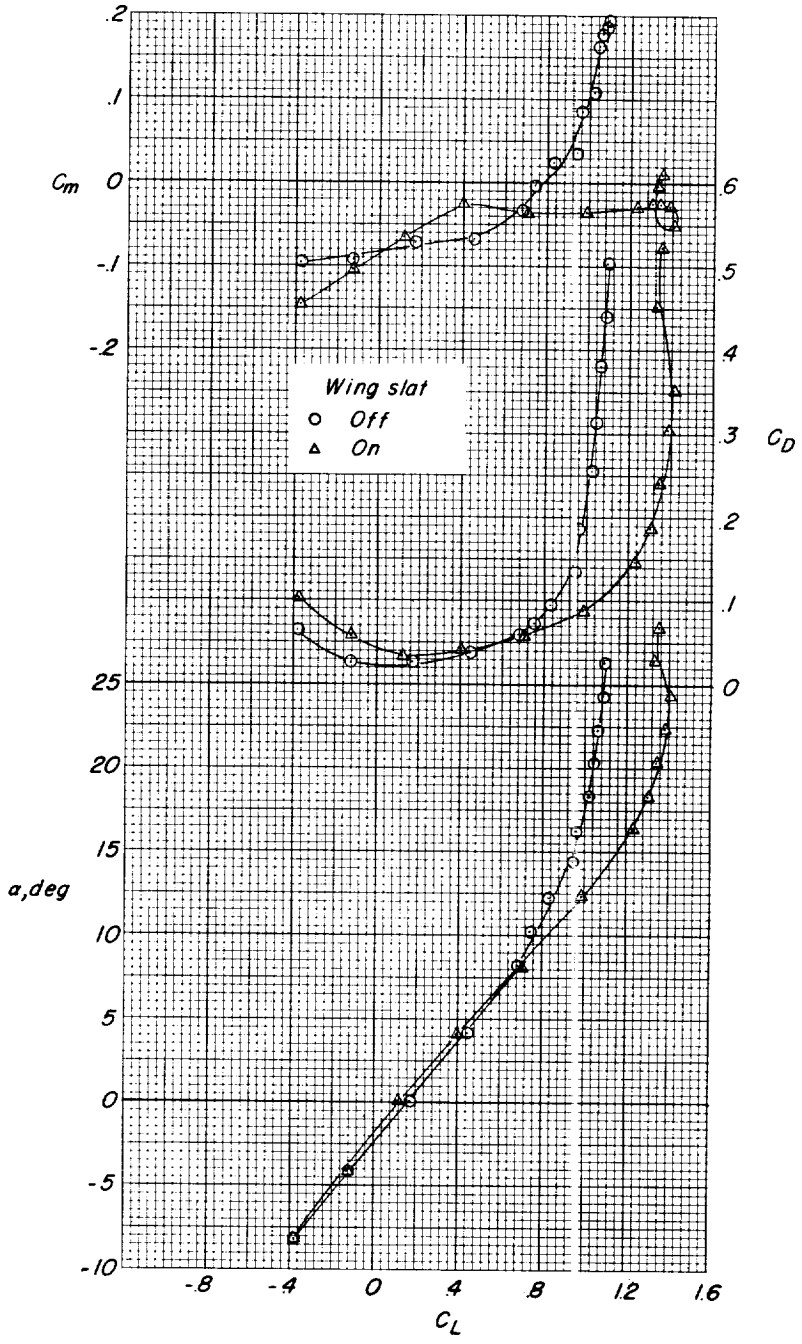

(a) $\delta_f = 0^o$; stabilizer off; $h = -0.082\bar{c}$.

Figure 7.- Effect of wing leading-edge slat on the aerodynamic characteristics of the model. Slat span = 0.57 $\frac{b}{2}$; $\delta_s = 42^o$; $C_{\mu,w} = 0$.

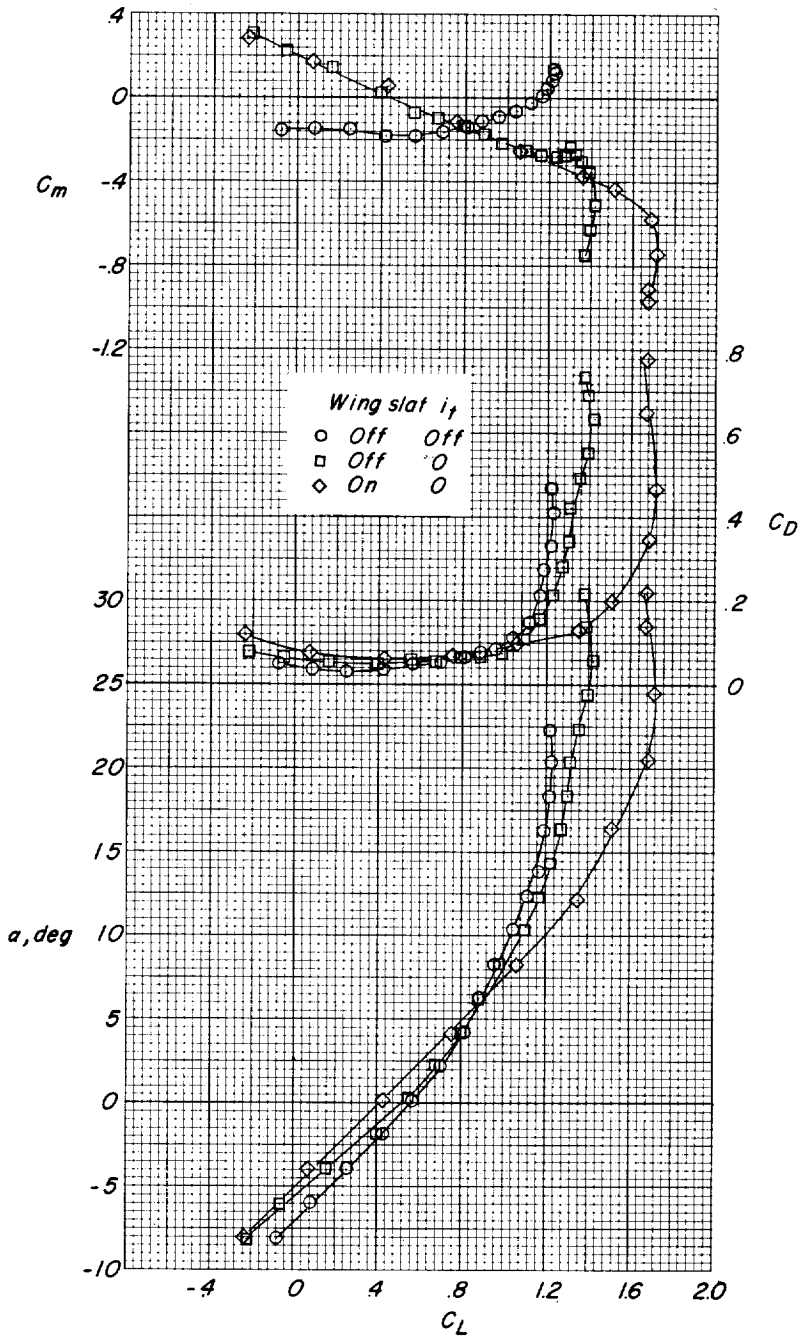

(b) $\delta_f = 13^o$; $z = 0.928\bar{c}$; $h = -0.082\bar{c}$.

Figure 7.- Concluded.

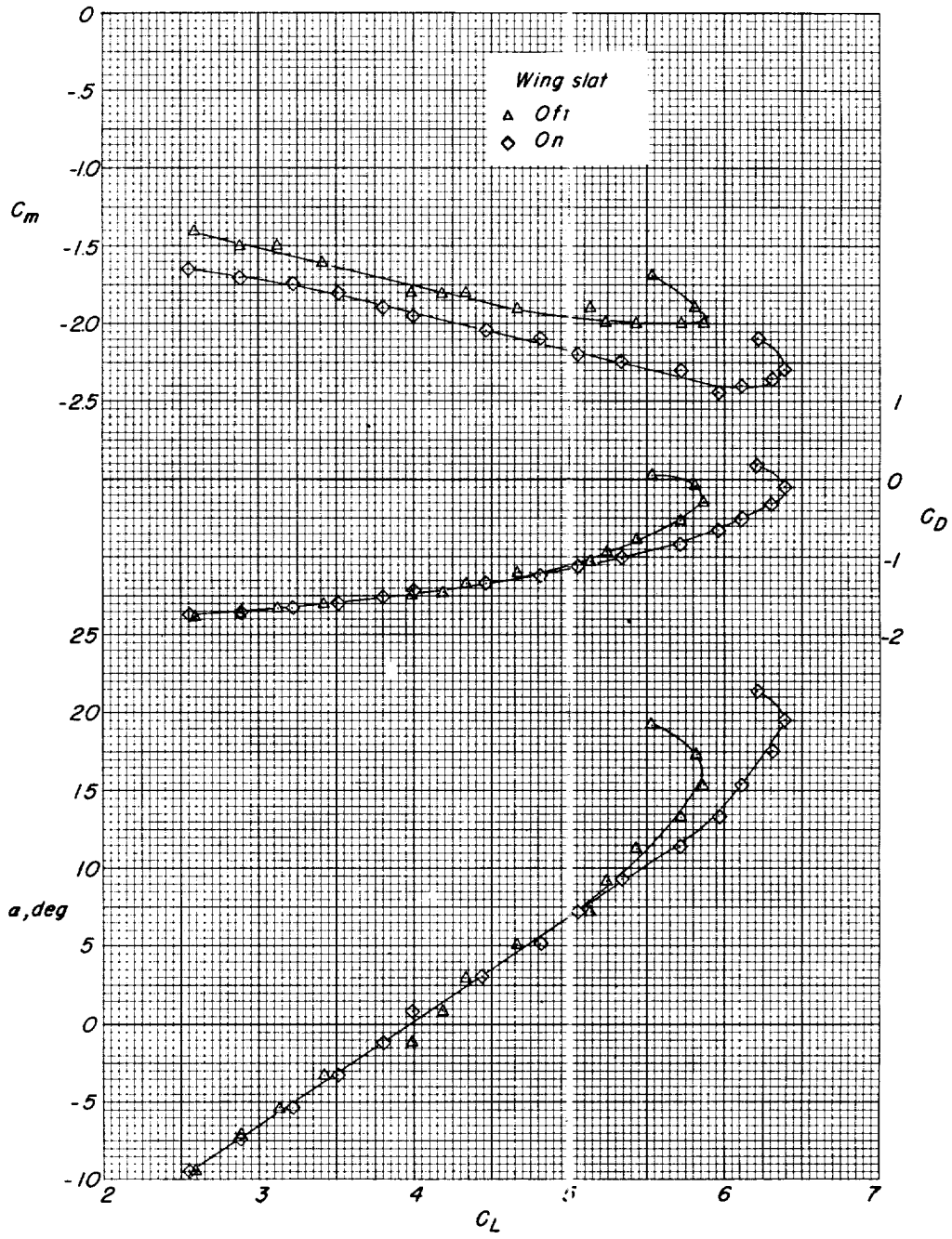

(a) $\delta_f = 21^\circ$; $\delta_s = 42^\circ$; $C_{\mu,w} = 3.09$; slat span = 0.40 $\frac{b}{2}$; h = 0.062$\bar{c}$.

Figure 8.- Effect of wing leading-edge slat on the aerodynamic characteristics of the model with stabilizer off.

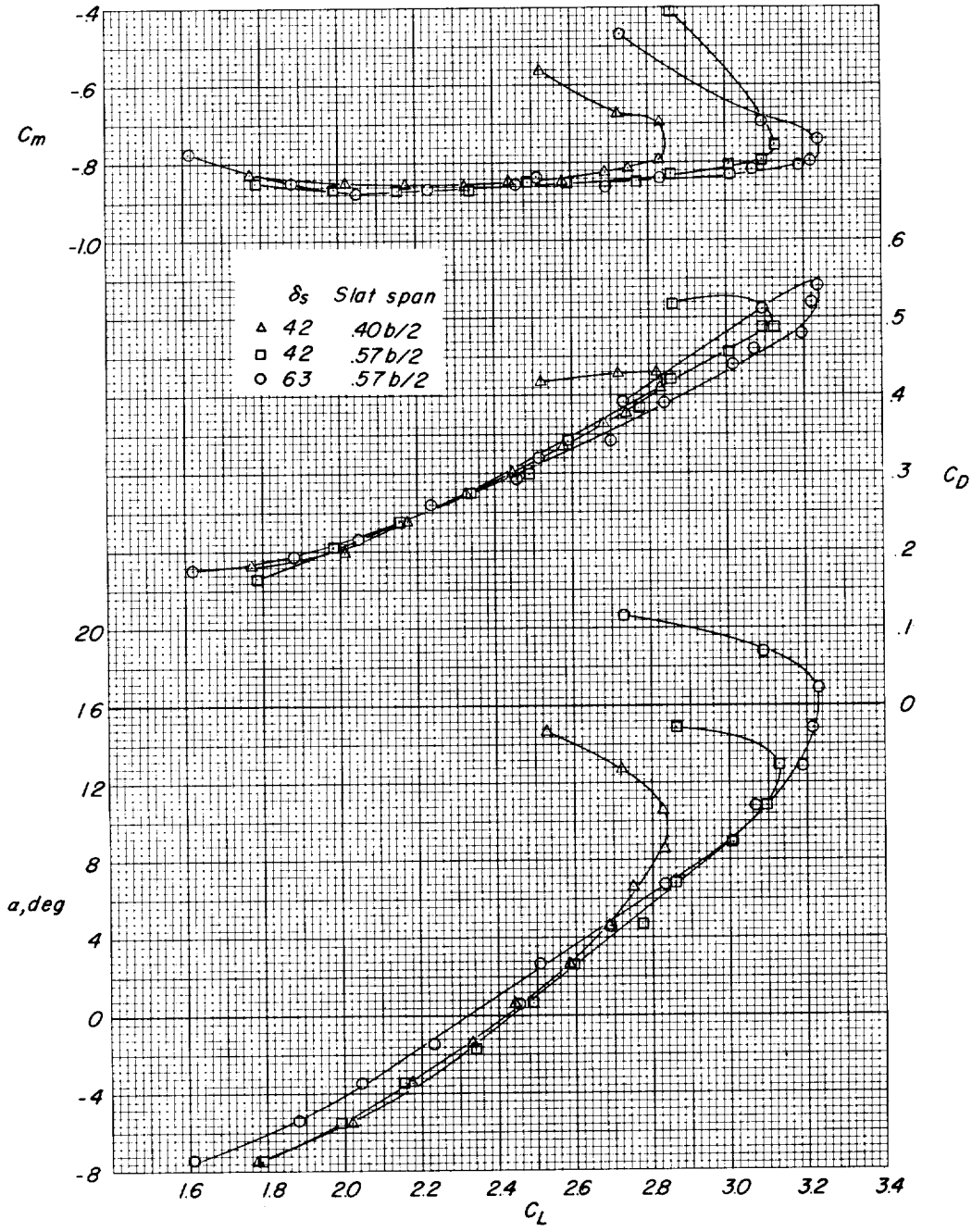

(b) $\delta_f = 57^\circ$; $C_{\mu,w} = 0.1$; $h = 0.062\bar{c}$.

Figure 8.- Continued.

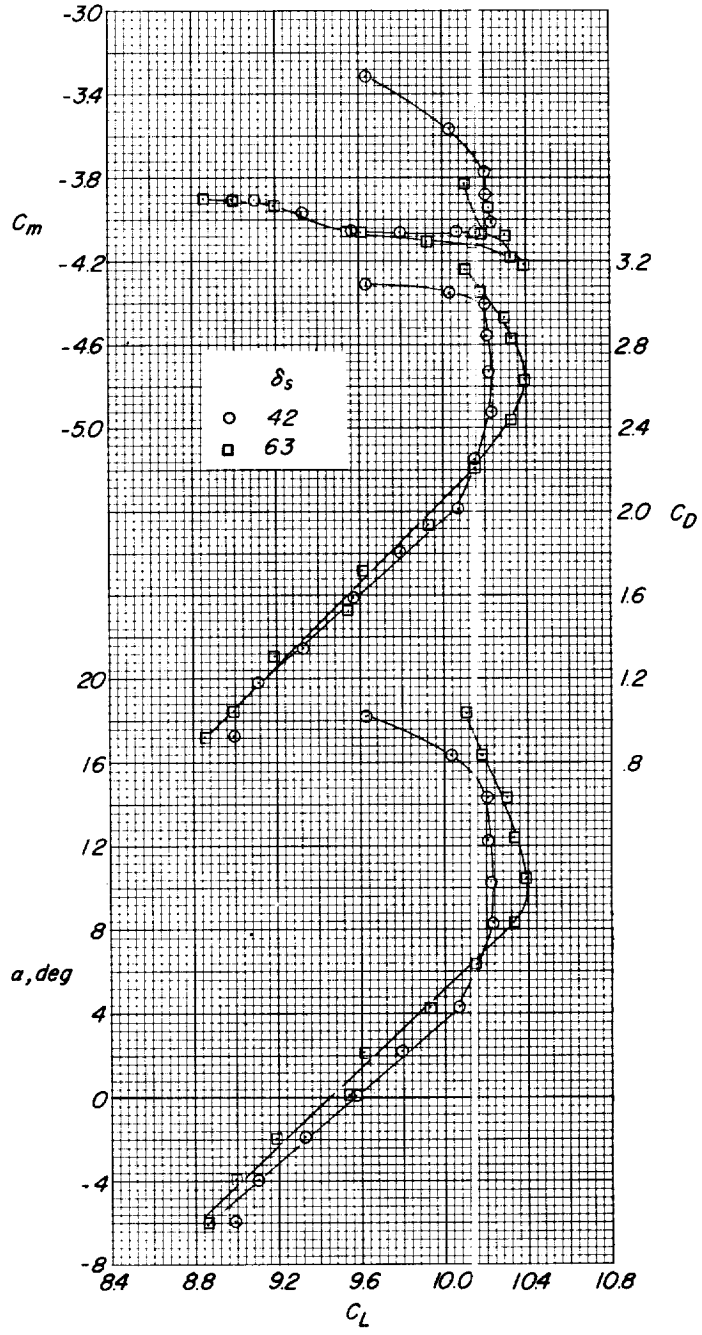

(c) $\delta_f = 70^\circ$; $C_{\mu,w} = 3.02$; slat span = $0.57\ \frac{b}{2}$; $h = -0.082\bar{c}$.

Figure 8.- Concluded.

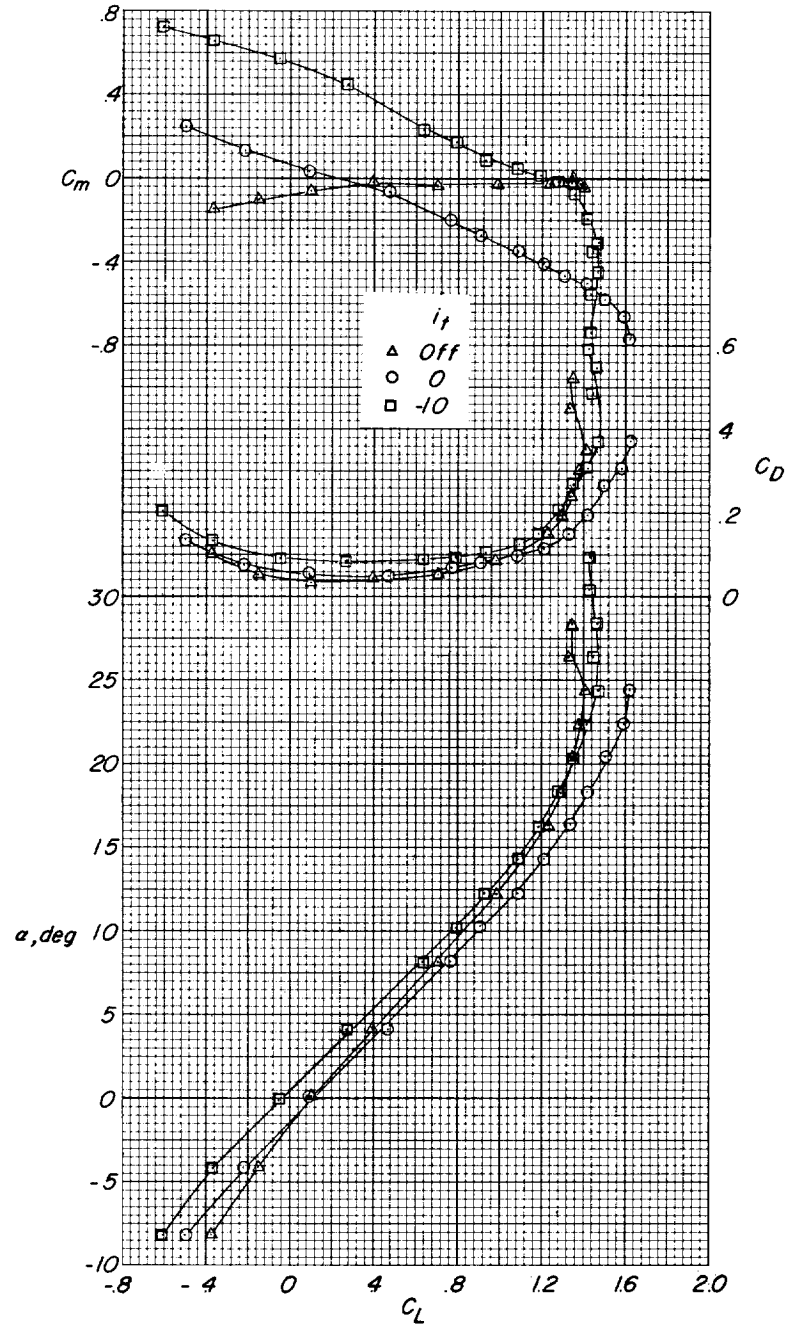

(a) $C_{\mu,w} = 0$.

Figure 9.- Aerodynamic characteristics for the stabilizer. $\delta_f = 0^o$; $z = 0.928$; slat span = $0.57 \frac{b}{2}$; $\delta_s = 42^o$; $h = -0.082\bar{c}$.

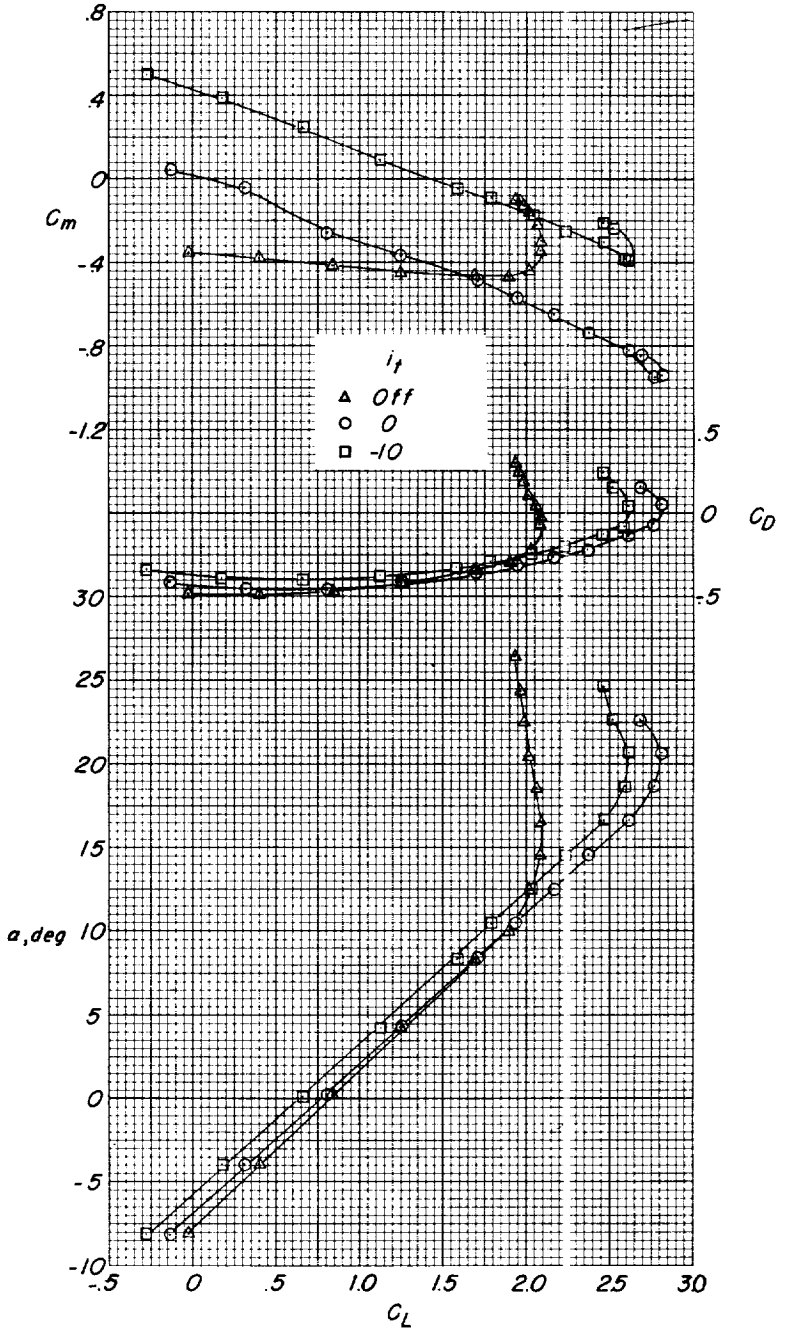

(b) $C_{\mu,w} = 0.78$.

Figure 9.- Continued.

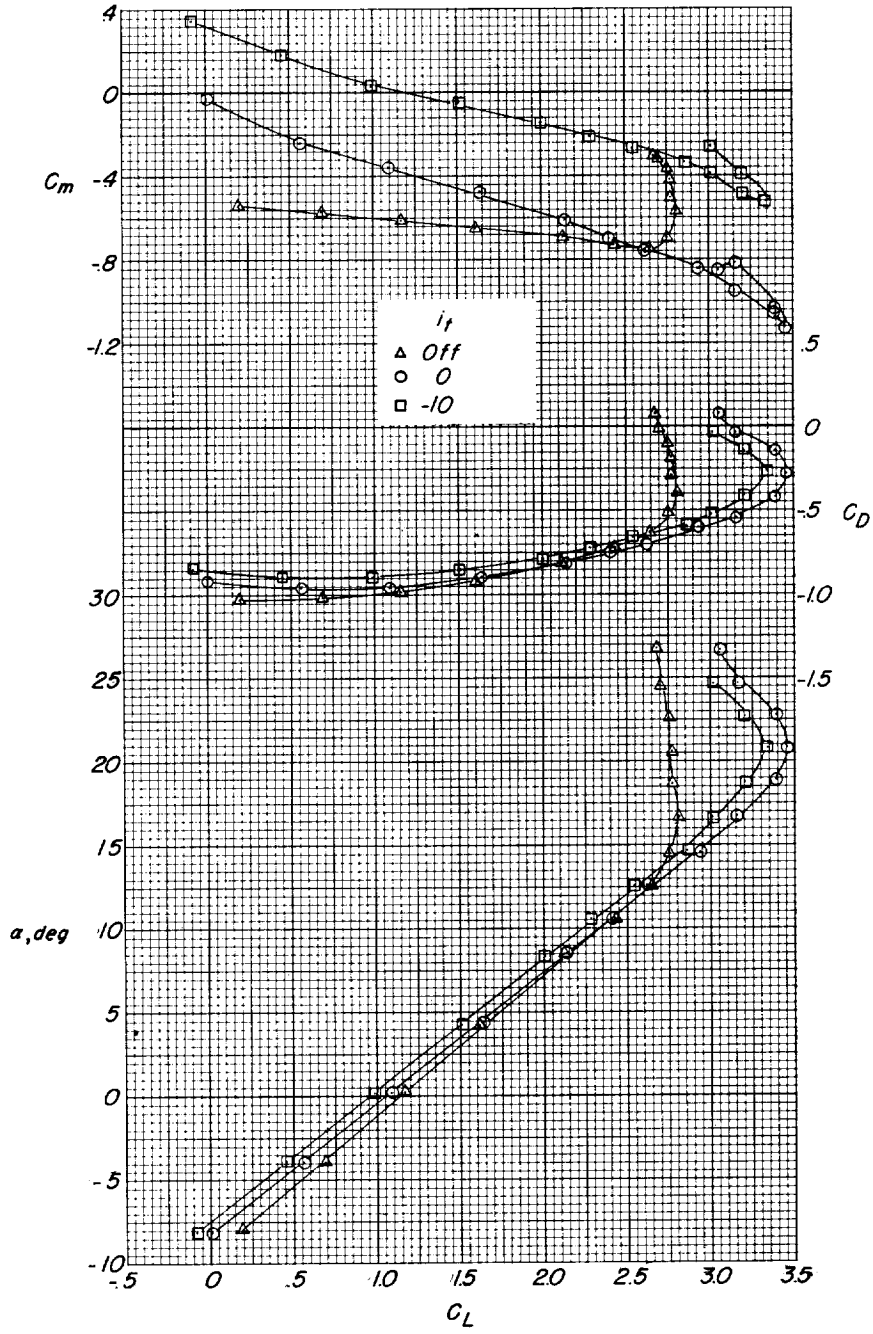

(c) $C_{\mu,w} = 1.56$.

Figure 9.- Continued.

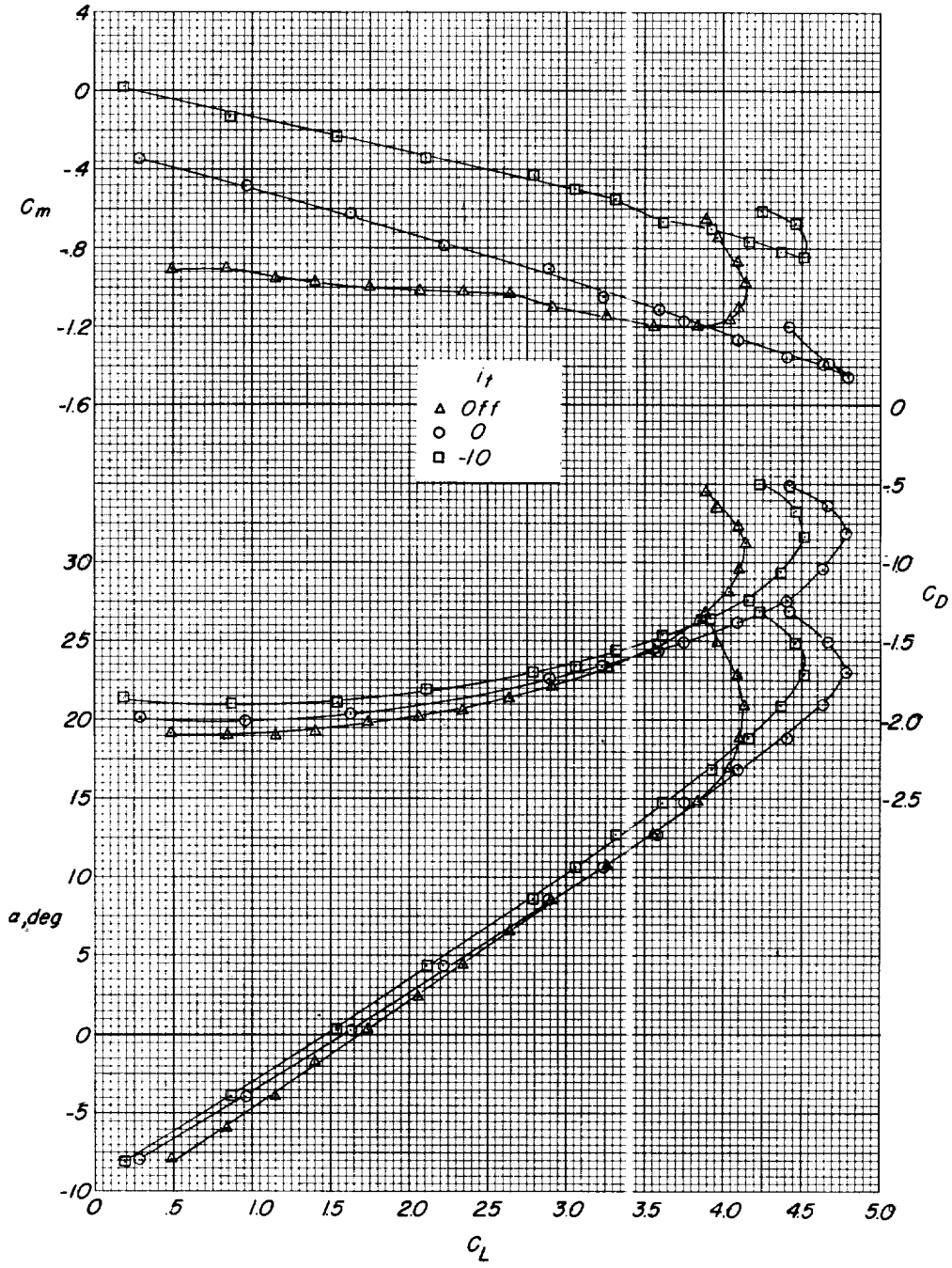

(d) $C_{\mu,w} = 3.13$.

Figure 9.- Concluded.

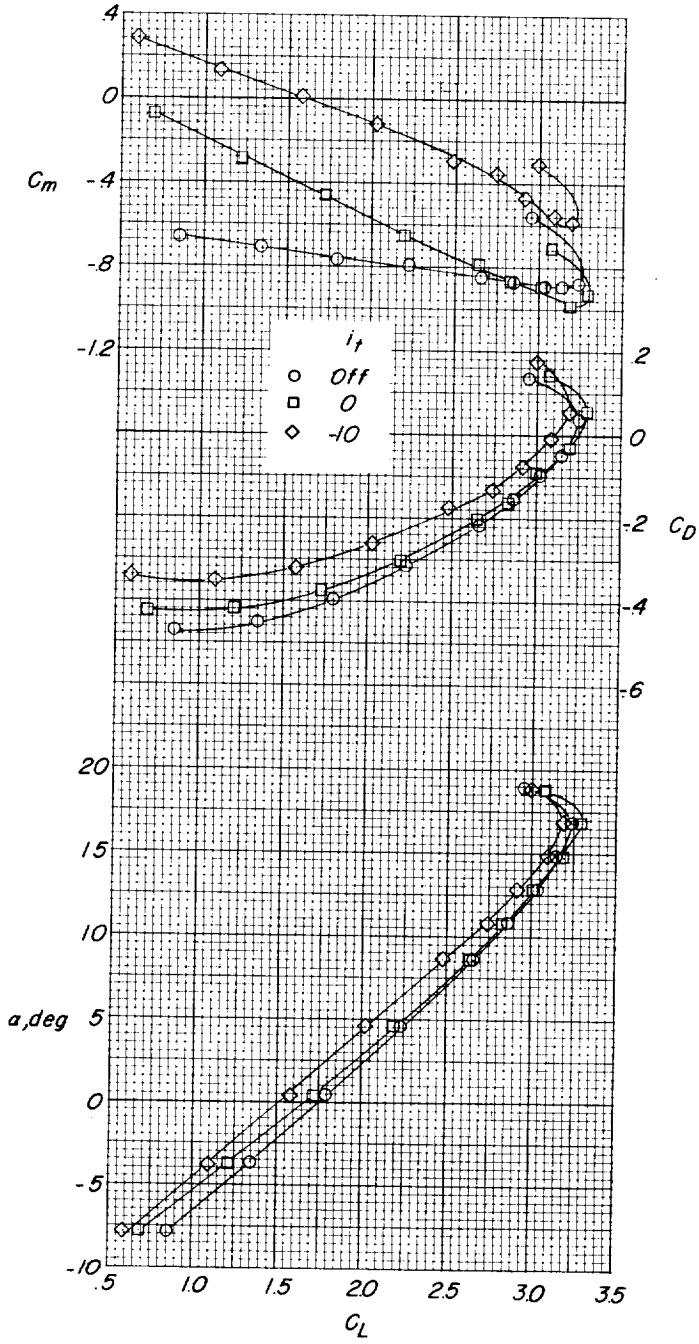

(a) $C_{\mu,w} = 0.77$.

Figure 10.- Aerodynamic characteristics for the stabilizer. $\delta_f = 13^\circ$; $z = 0.928$; $h = -0.082\bar{c}$; slat span = $0.57\ \frac{b}{2}$; $\delta_s = 42^\circ$.

32

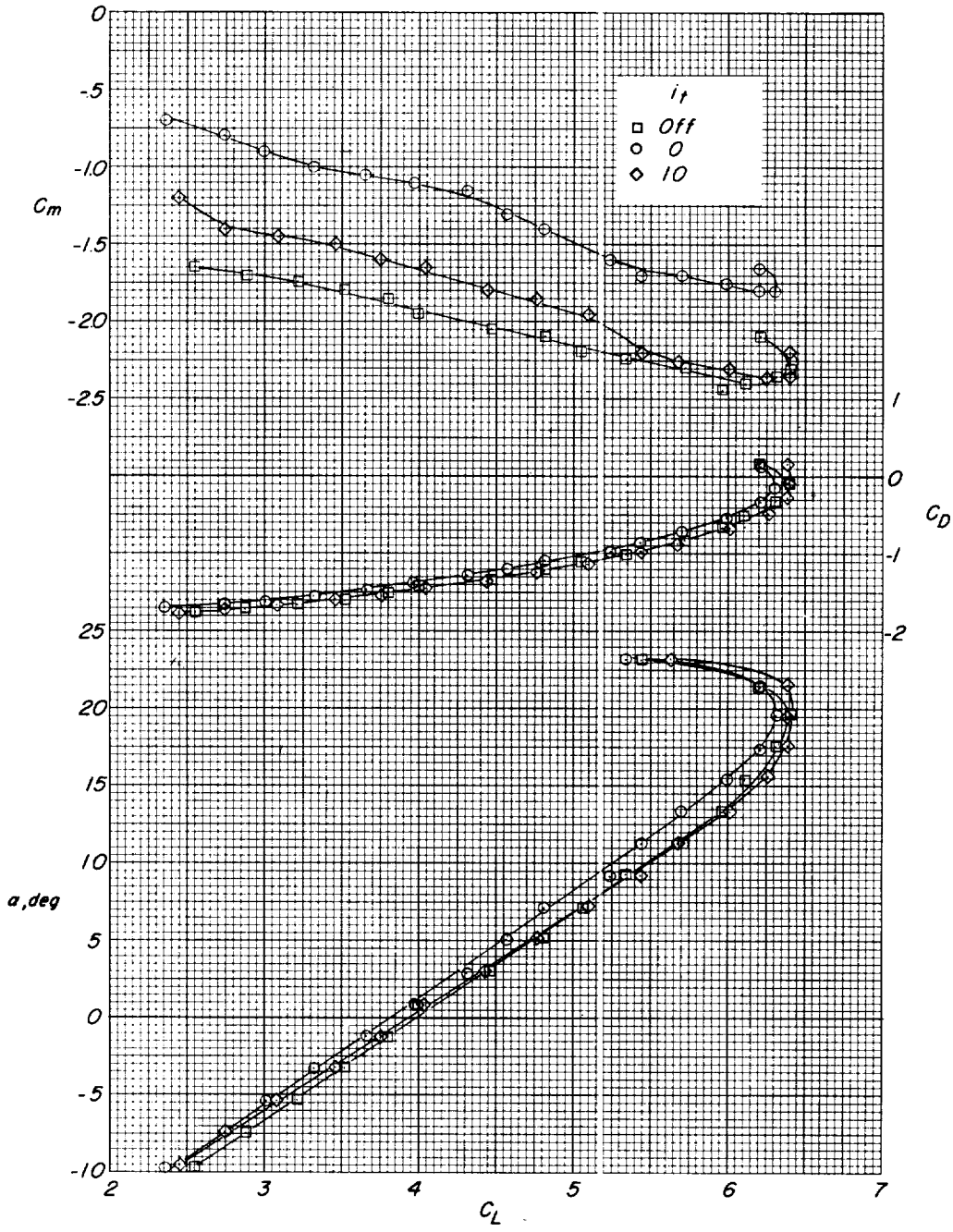

Figure 11.- Aerodynamic characteristics for the stabilizer with wing flap deflected 21°. $C_{\mu,w}$ = 3.09; slat span = 0.40 $\frac{b}{2}$; δ_s = 42°; z = 0.928; h = 0.062$\bar{c}$.

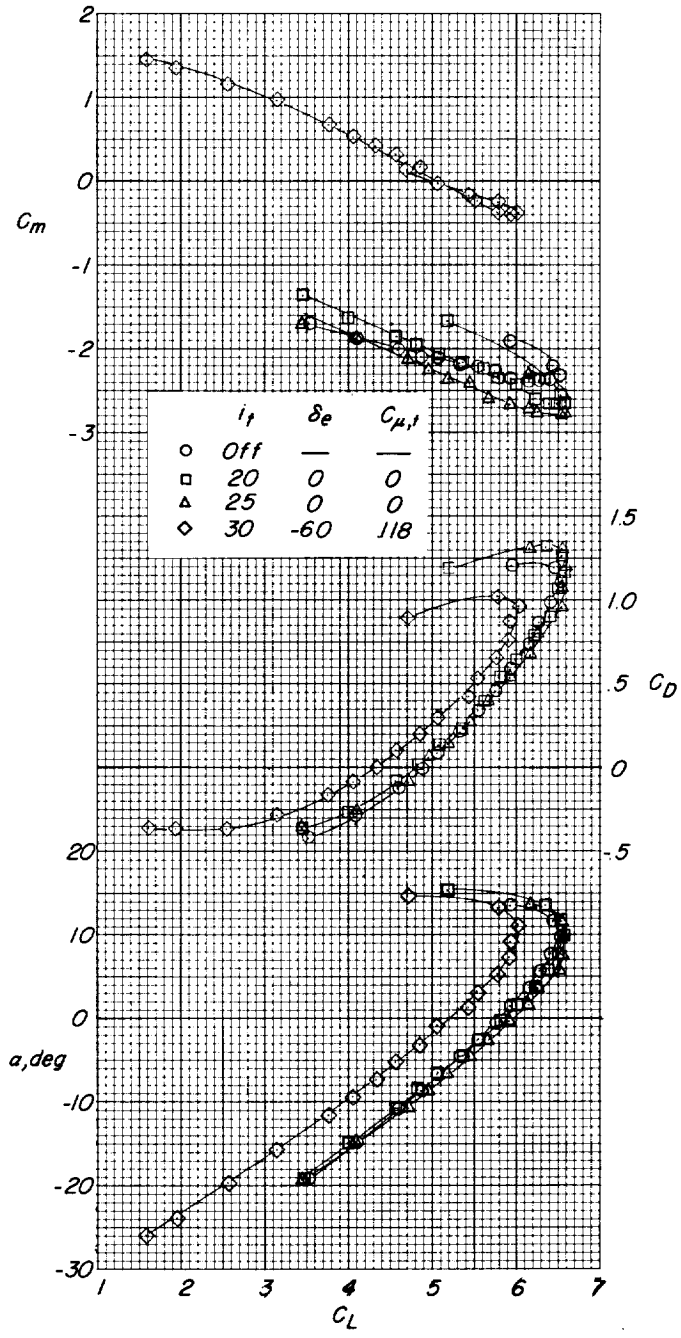

(a) $C_{\mu,w} = 1.55$.

Figure 12.- Aerodynamic characteristics for the stabilizer with wing flap deflected 57°; slat span = 0.40 $\frac{b}{2}$; δ_s = 42°; z = 0.928; h = 0.062$\bar{c}$.

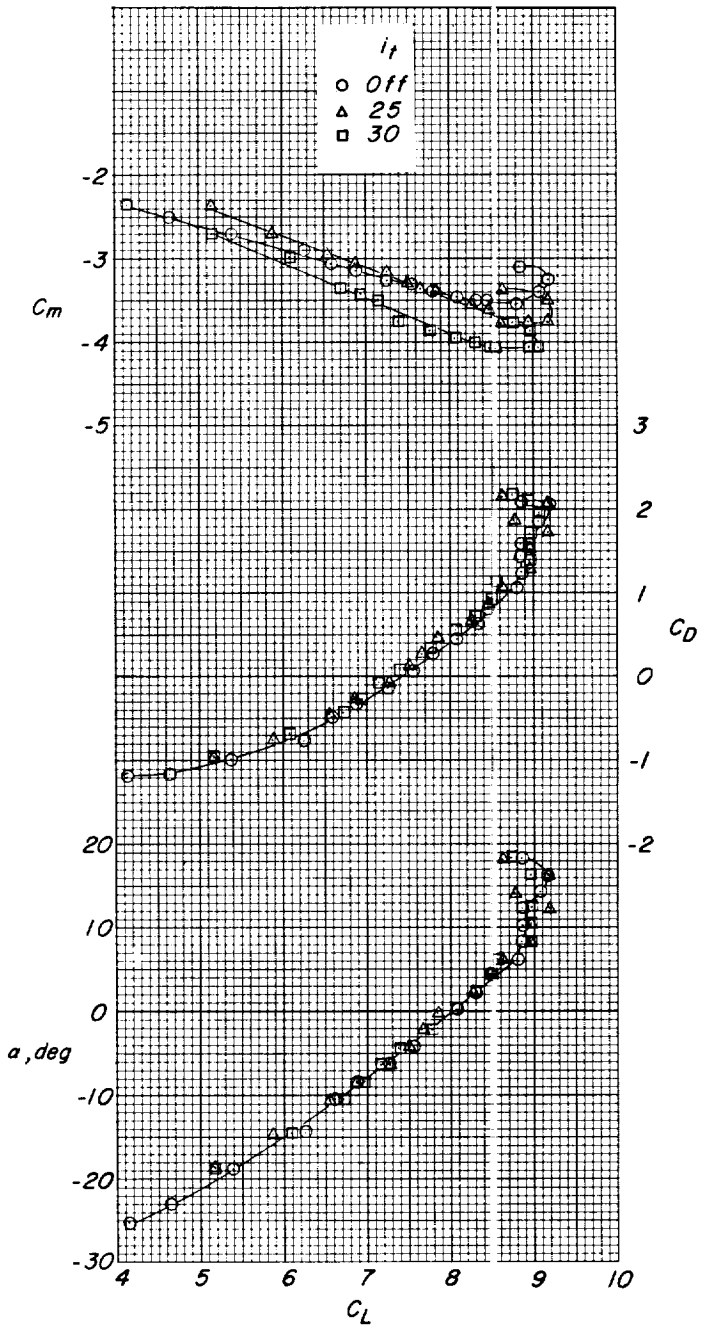

(b) $C_{\mu,w} = 3.09$.

Figure 12.- Concluded.

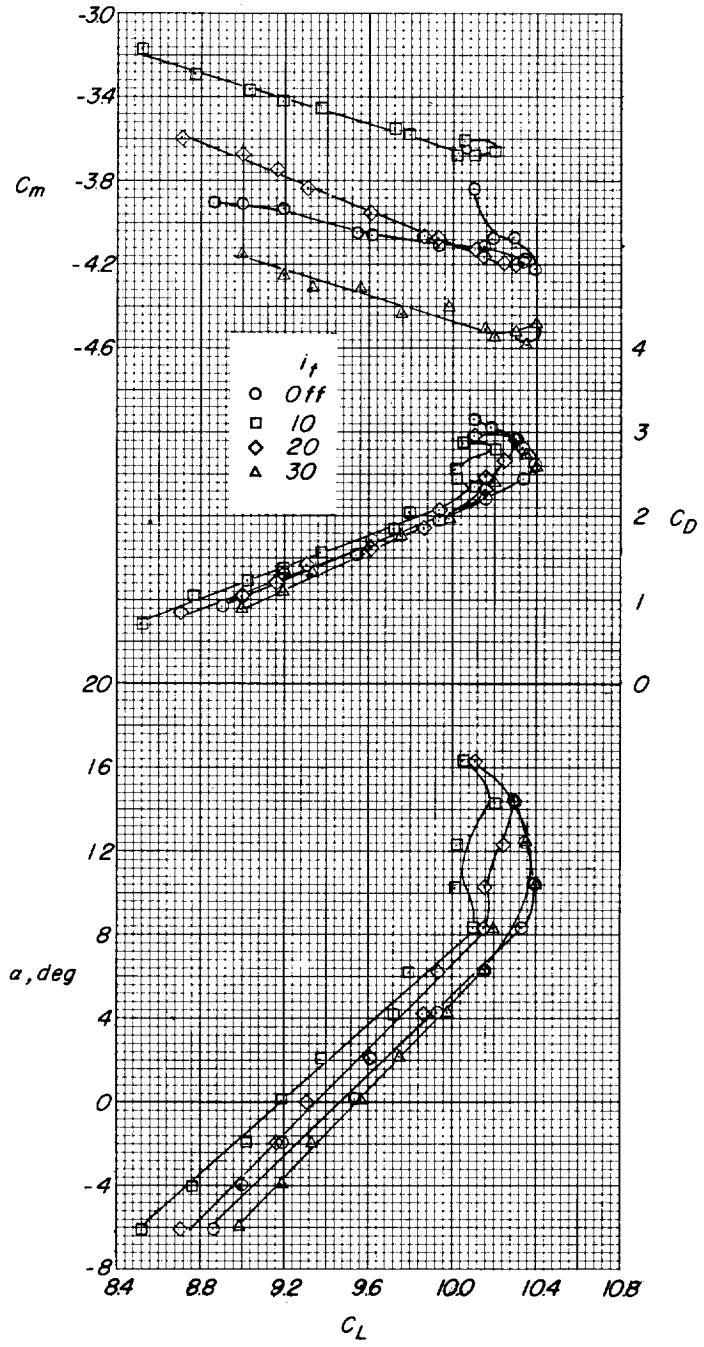

Figure 13.- Aerodynamic characteristics for the stabilizer with wing flap deflected 70°. $C_{\mu,w}$ = 3.02; slat span = 0.57 $\frac{b}{2}$; δ_s = 63°; z = 0.928; h = -0.082$\bar{c}$.

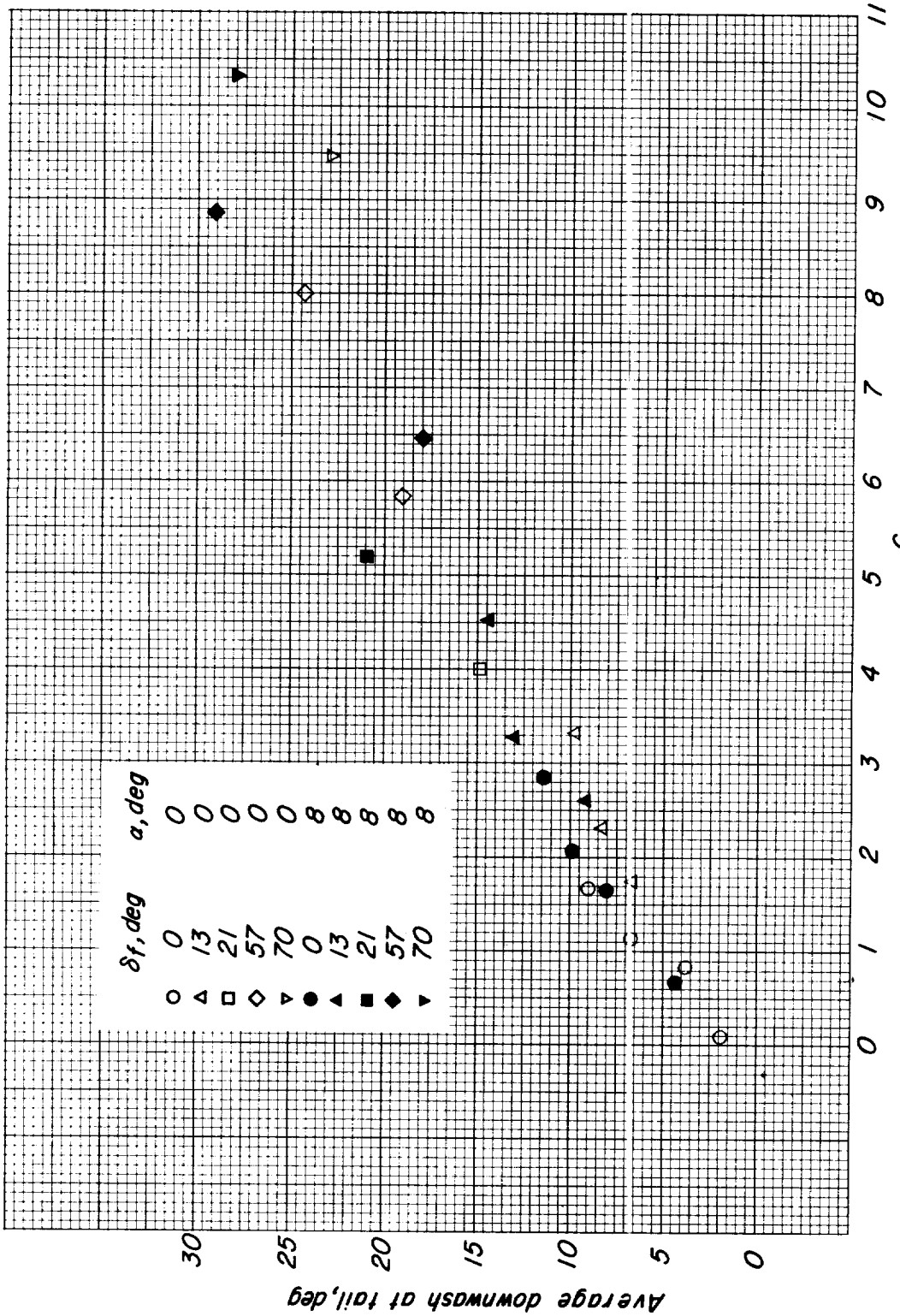

Figure 14.- Variation of average downwash at the tail with lift coefficient. z = 0.928c.

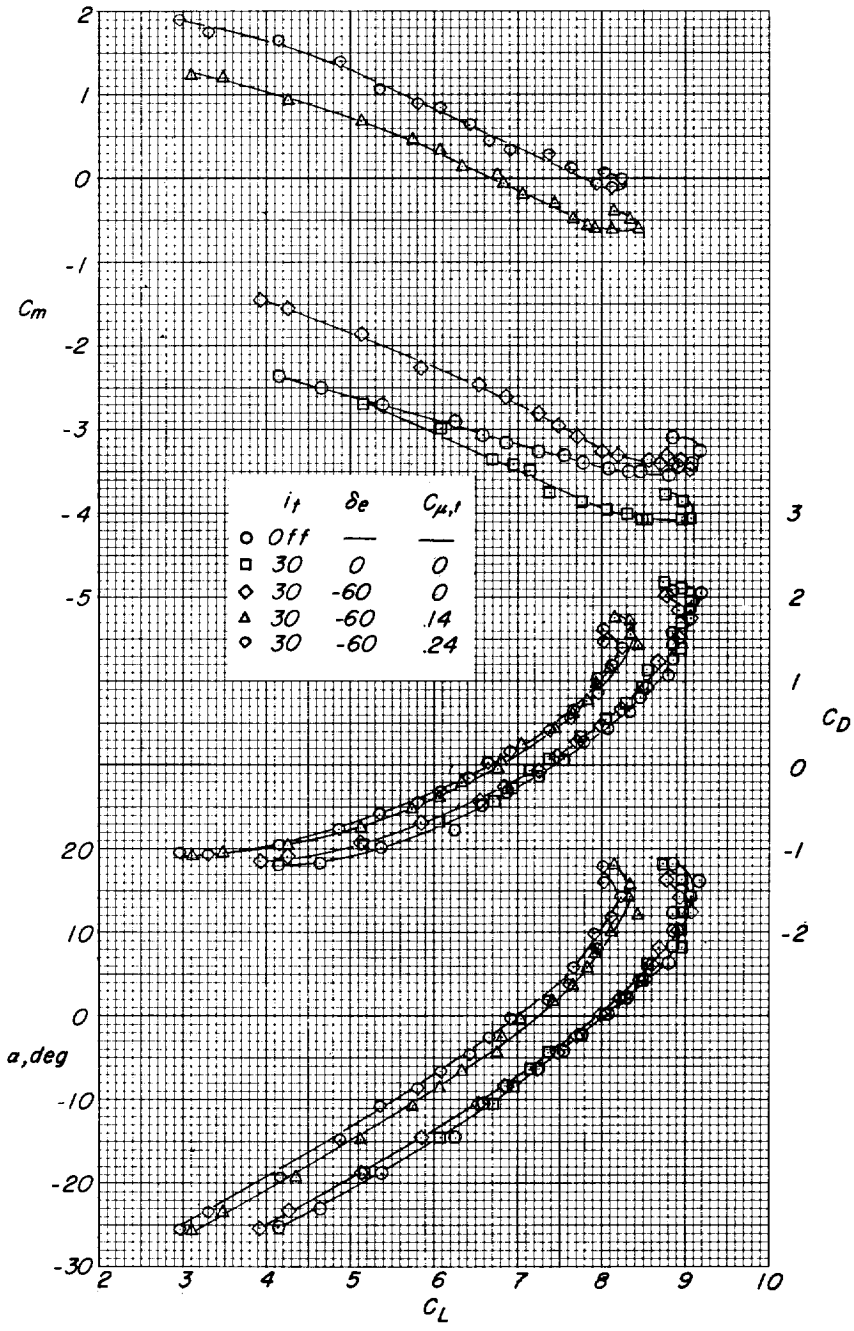

(a) $\delta_f = 57^\circ$; $\delta_s = 42^\circ$; slat span = 0.40 $\frac{b}{2}$; h = 0.062$\bar{c}$.

Figure 15.- Aerodynamic characteristics of the model with blowing over the deflected elevator. z = 0.928; $C_{\mu,w} = 3.09$.

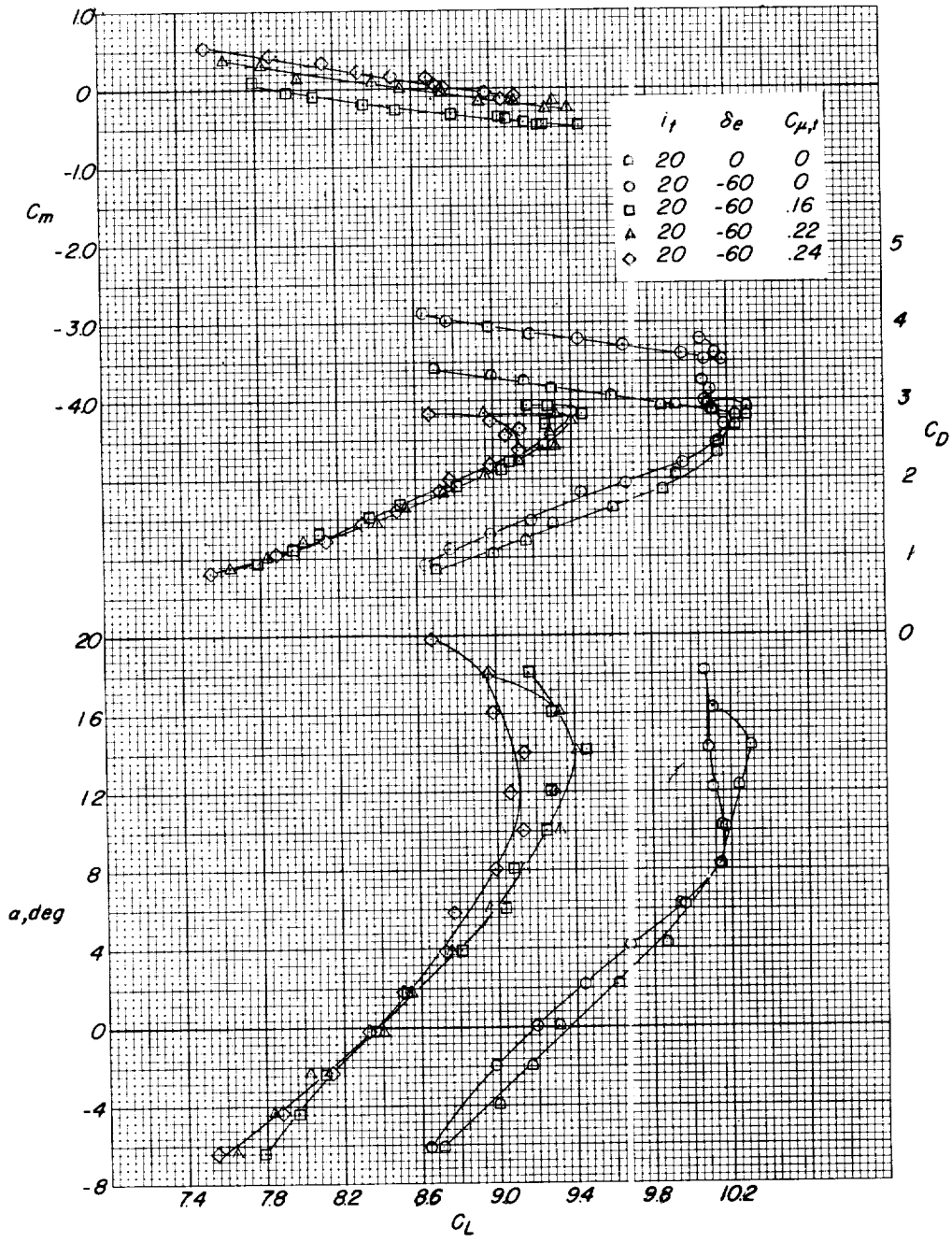

(b) $\delta_f = 70^\circ$; $\delta_s = 63^\circ$; slat span = 0.57 $\frac{b}{2}$; h = -0.082$\bar{c}$.

Figure 15.- Concluded.

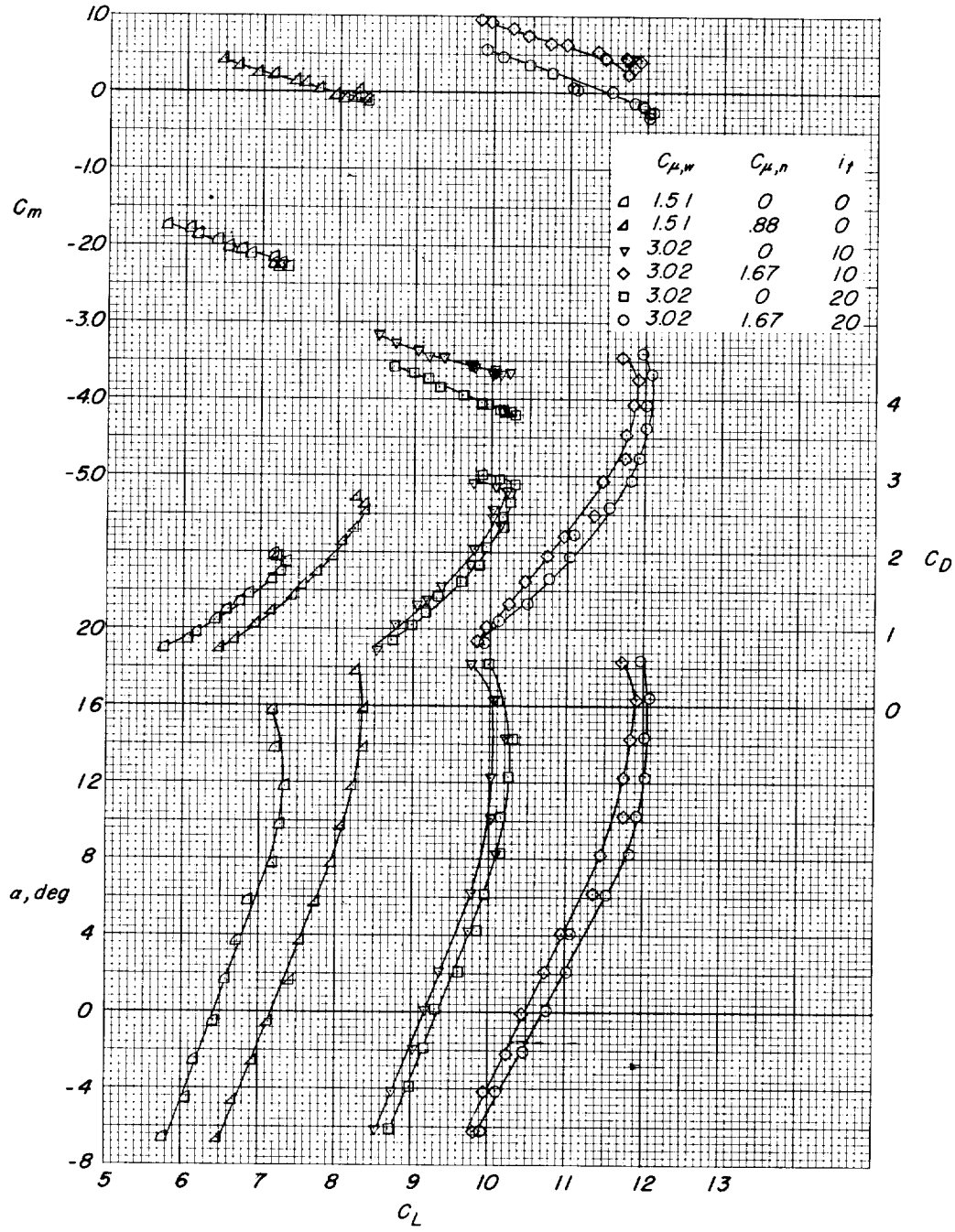

Figure 16.- Effects of a downward blowing nose jet on the longitudinal aerodynamic characteristics of the model. $\delta_f = 70^\circ$; nose jet moment arm = $2.4\bar{c}$; z = 0.928; $\delta_e = 0^\circ$; $\delta_s = 63^\circ$; slat span = 0.57 $\frac{b}{2}$; h = $-0.082\bar{c}$.

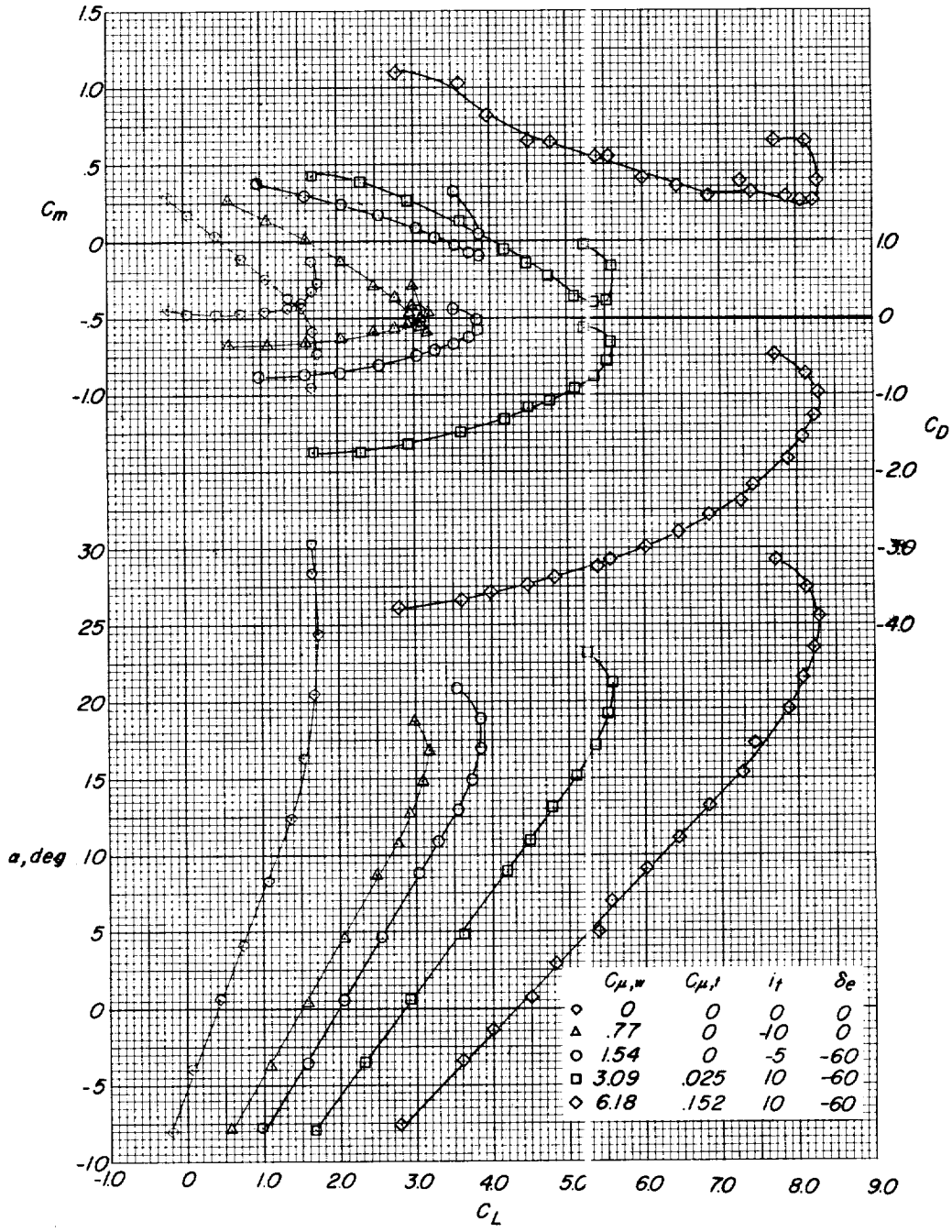

(a) $\delta_f = 13^\circ$; $\delta_s = 42^\circ$; slat span = 0.57 $\frac{b}{2}$; h = -0.082$\bar{c}$.

Figure 17.- Pitch characteristics for a range of trimmed lift coefficients. z = 0.928.

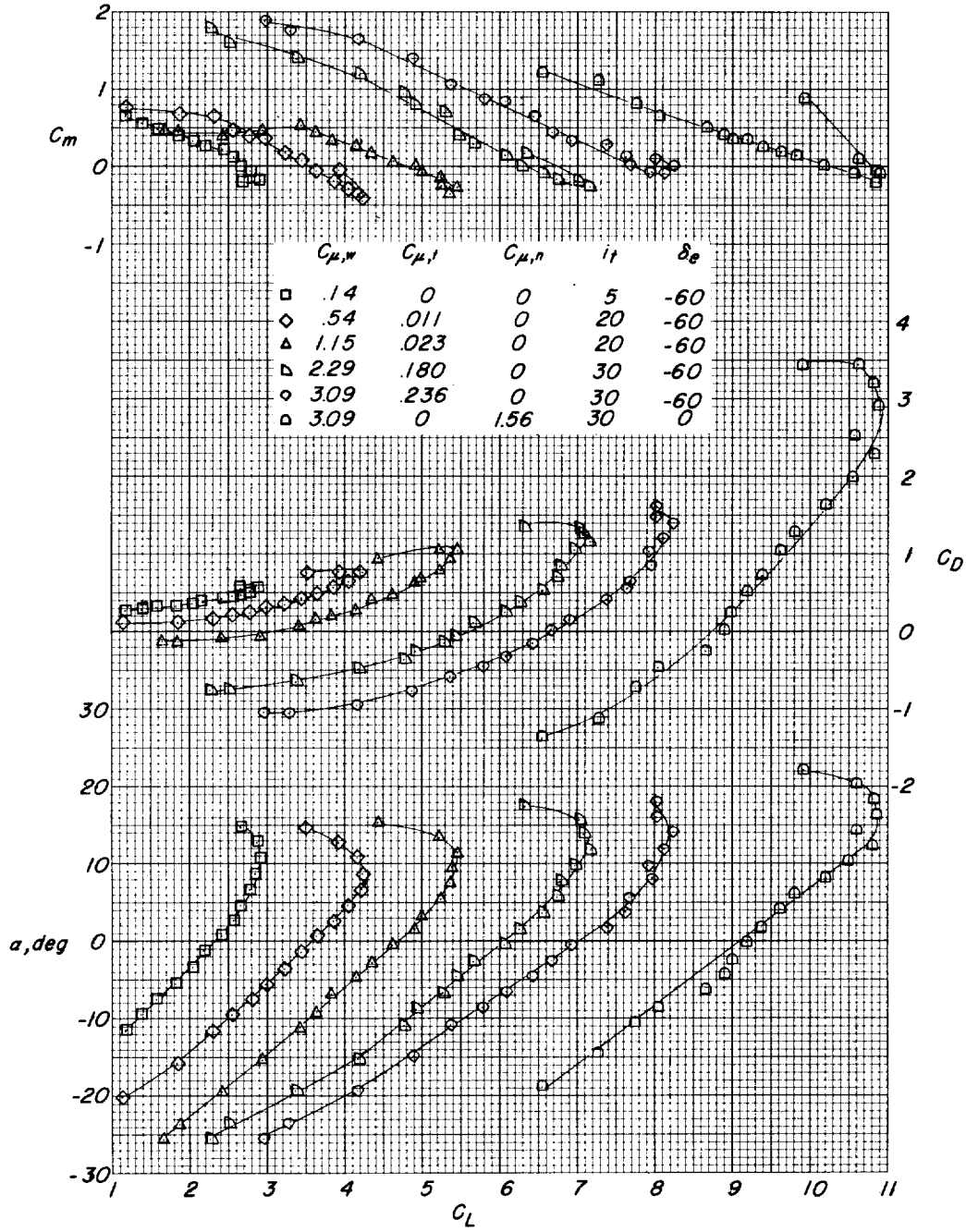

(b) $\delta_f = 57^\circ$; $\delta_s = 42^\circ$; slat span = 0.40 $\frac{b}{2}$; h = 0.062$\bar{c}$.

Figure 17.- Continued.

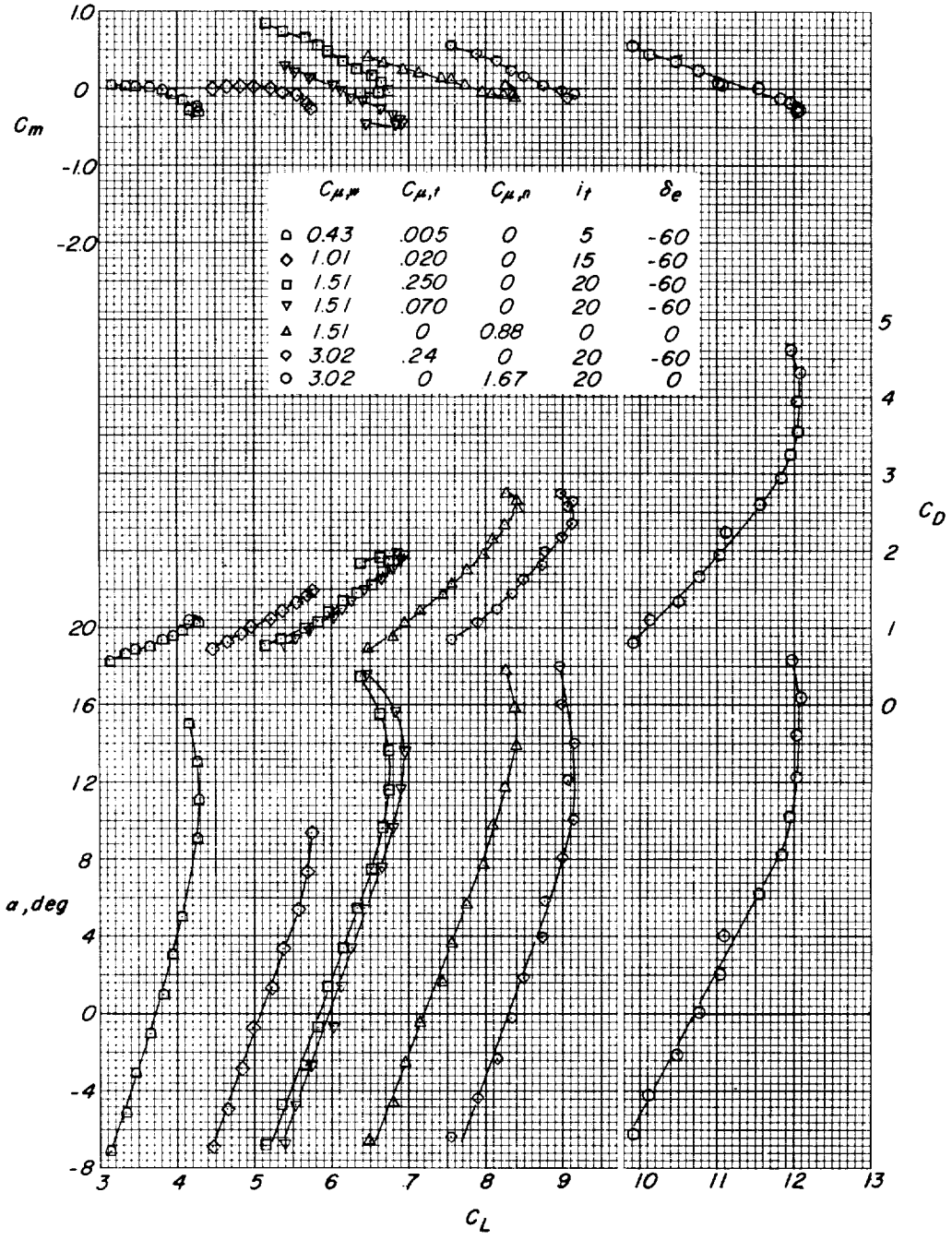

(c) $\delta_f = 70^\circ$; $\delta_s = 63^\circ$; slat span = 0.57 $\frac{b}{2}$; h = -0.082$\bar{c}$.

Figure 17.- Concluded.

L-931